December 2019

Role of Regulatory T Cells in the Development and Progression of Lyme Disease in Balb/c Mice

Kaitlyn Nielsen
University of Wisconsin-Milwaukee

ROLE OF REGULATORY T CELLS IN THE DEVELOPMENT AND PROGRESSION OF LYME DISEASE IN BALB/C MICE

by

Kaitlyn N. Nielsen

A Thesis Submitted in

Partial Fulfillment of the

Requirements for the Degree of

Master of Science

in Biomedical Sciences

at

The University of Wisconsin-Milwaukee

December 2019

ABSTRACT

ROLE OF REGULATORY T CELLS IN THE DEVELOPMENT AND
PROGRESSION OF LYME DISEASE IN BALB/C MICE

by

Kaitlyn N. Nielsen

The University of Wisconsin-Milwaukee, 2019
Under the Supervision of Professor Dean T. Nardelli

Lyme disease, caused by *Borrelia burgdorferi*, is an increasingly important public health concern, with tens of thousands of new cases being diagnosed each year, even in previously non-endemic areas. It is known that symptoms of Lyme disease are caused by an inflammatory immune response initiated to aid in clearance of the pathogen. Left unchecked, these inflammatory responses can potentially increase tissue damage, leading to increased disease severity. Mechanisms responsible for the control of the inflammatory response to infection with *B. burgdorferi* are not entirely understood. Evidence exists that regulatory T (Treg) cells, a population of Foxp3-expressing CD4$^+$ T cells known to play a vital role in controlling the immune response, may be important in reducing disease associated with *B. burgdorferi* infection. However, the role of Treg cells in host response to *B. burgdorferi* has not been examined fully. Here, we hypothesized that Treg cells control the development and progression of Lyme disease following *B. burgdorferi* infection. To test this hypothesis, two specific aims were addressed: (1) determine the effect of Treg cells on the development of arthritis following infection with *B. burgdorferi*; and (2) determine the effect of Treg cells on the control of the immune

response following infection with *B. burgdorferi*. Using a mouse model that allows for specific depletion of Treg cells, we demonstrate that depletion of Treg cells immediately prior to infection with *B. burgdorferi* leads to significantly increased edema in the tibiotarsal joints of mice infected with a low dose of organisms. We also provide evidence that Treg cell depletion affects the ability of the immune system to prevent bacterial dissemination. Depletion of Treg cells appeared not to have an effect on the development of arthritis at the low doses of infection we used, despite the increased tibiotarsal joint swelling. Several weeks after infection, increased levels of IL-10 were observed in the serum of mice previously depleted of Treg cells. Collectively, these findings provide partial support for the hypothesis. Treg cell depletion prior to infection could potentially impact the induction of the initial immune response to *B. burgdorferi*, which could then have subsequent downstream effects on the development of disease; however, further studies are needed to test this hypothesis.

TABLE OF CONTENTS

LIST OF FIGURES

LIST OF TABLES

LIST OF ABBREVIATIONS

APC: allophycocyanin

BSK: Barbour-Stoenner-Kelly

CDC: Centers for Disease Control

DEREG: depletion of regulatory T cell

DMEM: Dulbecco's Modified Eagle's Medium

DTx: diphtheria toxin

EDTA: Ethylenediamine tetraacetic acid

ELISA: Enzyme-linked immunosorbent assay

EM: erythema migrans

FITC: fluorescein isothiocyanate

Foxp3: forkhead box p3

HCl: hydrochloric acid

IFN-γ: interferon-gamma

IL-4: interleukin-4

IL-5: interleukin-5

IL-10: interleukin-10

IL-17: interleukin-17

NaOH: sodium hydroxide

NapA: Neutrophil activating protein A

NMS: normal mouse serum

OspA: outer surface protein A

OspC: outer surface protein C

PBS: phosphate-buffered saline

PCR: polymerase chain reaction

PE: phycoerythrin

SEM: standard error of the mean

TGF-β: transforming growth factor beta

Th1: T-helper type 1 cell

Th2: T-helper type 2 cell

Th17: T-helper type 17 cell

Treg: Regulatory T cell

v/v: volume per volume

WT: wild-type

ACKNOWLEDGEMENTS

First and foremost, I would like to express my sincerest gratitude to my advisor, Dr. Dean Nardelli, for his continuous patience, encouragement, and support throughout my time as a graduate student. The knowledge he has imparted and his advice and guidance have been vital to both the research and the writing of this thesis. I could not have asked for a better mentor and I am truly grateful to have been given the opportunity to work in his lab. I would like to express my gratitude to Dr. Elizabeth Liedhegner for her advice and support, as well as her assistance with training and practicing new laboratory techniques with me and her assistance with troubleshooting any problems I encountered during my research. I would also like to thank my final committee member, Dr. Jennifer Doll, for her insight and valuable feedback which have helped me to continuously improve both my writing and presenting skills. Additionally, I would like to thank my fellow lab member and classmate, Tanya, not only for her collaboration and teamwork, but also for our scientific discussions, and her feedback and support. Last, but not least, I would like to thank my wonderful family, friends, and boyfriend for their continuous love and support, and for listening to all of my complaints and stressed rants over the years.

CHAPTER 1: INTRODUCTION

I. Background

Lyme Borreliosis

Lyme borreliosis, more commonly known as Lyme disease, is the most common vector-borne infection in the United States, with approximately 30,000 new cases being reported each year and an estimated 300,000 individuals predicted to acquire it per year (Centers for Disease Control and Prevention 2019). In 2014, The CDC named Lyme disease the fifth most common "Nationally Notifiable Disease" (Adams *et al*. 2016). Initial symptoms of Lyme disease include general flu-like symptoms usually associated with a characteristic "bull's-eye" rash at the site of infection (Nau *et al*. 2009). As infection progresses, the microorganisms spread to other organs, such as the heart, brain, or joints (Nau *et al*. 2009). Although this disease is typically not considered to be life threatening, it can significantly affect the quality of life of those infected, making this disease an important public health concern.

The causative agent of Lyme disease in the United States is the spirochete *Borrelia burgdorferi* (Steere *et al*. 2004). Discovered in 1982 by Wilhelm Burgdorfer (Burgdorfer *et al*. 1982), this highly motile extracellular bacterium is not known to produce toxins but possesses a variety of virulence factors which enable it to colonize hosts, migrate through tissues by adhering to host cells, and evade the immune response (Steere *et al*. 2004). Of particular interest is the ability of this organism to adhere to a variety of host tissue components using many different cell surface proteins. *B. burgdorferi* has been shown to bind decorin (Guo *et al*. 1995), which is a proteoglycan found abundantly on

collagen fibers in the skin and joints, using decorin-binding proteins A and B (DbpA and DbpB). *B. burgdorferi* has also been shown to bind fibronectin (Probert and Johnson 1998), which is a major component of the extracellular matrix and is found in a variety of tissues and organs, using the fibronectin-binding protein (BBK32). *B. burgdorferi* can also establish infection by evading the immune response. This organism is able to bind Factor H (Hellwage *et al.* 2001), which is responsible for regulating the alternative complement pathway via C3b, a vital host complement component. The ability of the organism to bind Factor H facilitates with its subsequent inactivation; thus, binding of Factor H inhibits bacterial destruction by complement-mediated killing. These abilities allow the organism to colonize the host and effectively establish infection.

Transmission of B. burgdorferi

B. burgdorferi is transmitted via the bite of the tick *Ixodes scapularis* (deer tick) or *Ixodes pacificus* (black-legged tick). *I. scapularis* is the primary vector in the Northeastern and upper Midwest regions of the United States, whereas *I. pacificus* is the primary vector in the Western region of the United States (Stanek *et al.* 2011). In areas where these ticks are endemic, Lyme disease is traditionally prevalent as well. While many animals, including birds and rodents, can act as hosts for these ticks, the white-tailed deer is one of the most common hosts as its large size allows for the transport and support of many ticks at once (Stanek *et al.* 2011). Although the life cycle of these ticks consists of four stages, the nymph stage is primarily responsible for transmitting *B. burgdorferi*. Ticks must remain attached to the host for at least thirty-six hours to transmit *B. burgdorferi*; therefore, the small size of the nymph provides an advantage as it is less likely to be discovered and removed before transmission can

occur (Hubalek 2009). Most human infection occurs between May and September, when the nymph stage is particularly prevalent and humans are outdoors for extended periods of time in endemic areas (Hubalek 2009).

B. burgdorferi is transmitted via the bite of infected ticks. Ticks themselves become infected after ingesting blood from an infected animal. *B. burgdorferi* survives in the midgut of the tick until it is transferred to a subsequent host when the infected tick feeds. To facilitate its transmission to the mammalian host, *B. burgdorferi* alters the expression of its outer surface proteins. Outer surface protein A (OspA) expression is upregulated in the midgut of the tick (Schwan *et al.* 1995), demonstrating an important role for OspA in attachment and colonization of the tick midgut (Pal *et al.* 2000). Upon feeding, the expression of OspA is downregulated, which allows for the migration of *B. burgdorferi* from the tick midgut to the salivary glands. This downregulation of OspA expression correlates with an upregulation of OspC expression (Schwan and Piesman 2000), which is important for colonization of the mammalian host (Schwan *et al.* 1995) and is required for infectivity (Grimm *et al.* 2003; Tilly *et al.* 2006). This shift in surface protein expression is thought to be a result of changes in temperature, pH, and osmolarity within the midgut of the tick as the tick ingests the blood during feeding (Schwan and Piesman 2000).

Changing climate and animal host migration has been leading to the spread of disease-carrying vectors to other parts of the country, with Lyme disease cases beginning to appear outside of the previously endemic areas. Since the discovery of Lyme-disease-associated ticks in northwestern Wisconsin in the late 1960s, the infected ticks have

been carried south and east, allowing for an increasing geographic distribution across the state (Kugeler *et al.* 2015). Not only have the infected tick vectors spread across the state of Wisconsin, they are also expanding in other regions of the country, increasing the chances that humans will become exposed to this disease. Geographic expansion studies have demonstrated that from 1993 to 2012, the incidence of Lyme disease increased 320% in northeastern states and 250% in north central states (Kugeler *et al.* 2015). No vaccines currently exist to prevent humans from developing Lyme disease, making a more complete understanding of this disease relevant for human health.

Clinical Manifestations, Diagnosis, and Treatment of Lyme Disease

Untreated Lyme disease affects multiple body systems and typically progresses through three stages: early localized infection, early disseminated infection, and late persistent infection (Strle and Stanek 2009). Early localized infection occurs within days to weeks following the bite from an infected tick. Erythema migrans (EM), the characteristic "bull's-eye" rash that is a hallmark of Lyme disease, occurs in 70-80% of infected patients (Steere *et al.* 2004). The center of the rash occurs at the site of the tick bite, occasionally with intermittent areas of clearing and inflammation radiating out from the center as the bacteria spread. In the absence of the rash, other symptoms of early localized infection closely resemble the flu; thus, often leading to misdiagnosis. The early disseminated stage occurs weeks to months following infection and is characterized by the spread of *B. burgdorferi* to other organ systems. Clinical manifestations at this stage of infection may include additional disseminated EM

lesions, and musculoskeletal and neurological symptoms, as well as symptoms of carditis (Strle and Stanek 2009). Musculoskeletal symptoms include myalgia or arthralgia (Wright *et al.* 2012). One of the most common neurological symptoms of Lyme disease is facial palsy, in which one half of the face exhibits a drooping appearance indicative of paralysis caused by damage to the facial nerve (Hildenbrand *et al.* 2009). Neurological symptoms such as lymphocytic meningitis, encephalitis, numbness or tingling in the hands or feet, or nerve pain may also occur (Auwaerter *et al.* 2004). *B. burgdorferi* can also invade heart tissue, causing symptoms of carditis. Lyme carditis is characterized by atrioventricular block, which prevents the conduction of electrical impulses through the heart leading to arrhythmias (Fish *et al.* 2008). Additional symptoms of carditis include heart palpitations and the feelings of being light-headed or dizzy (Scheffold *et al.* 2015). The late persistent stage occurs months to years after infection and is generally characterized by the further spread of the bacteria to the joint tissue, contributing to the development of arthritis (Steere *et al.* 2004). Also present at this stage, although rare, are worsened neurological symptoms (Auwaerter *et al.* 2004). Lyme arthritis is the most common late-stage symptom of Lyme disease and primarily affects large joints such as the knee (Wright *et al.* 2012).

The presence of the EM rash is generally sufficient for diagnosing Lyme disease in areas where the disease is endemic. However, there are incidences in which the rash occurs in areas that are less visible or does not appear. Therefore, people may not realize they have been infected and will not seek medical treatment early during the course of infection. Lyme disease is diagnosed based on two-tiered serological testing. This testing is beneficial in the absence of the EM lesion or when the visible lesion does

not resemble the typical "bull's-eye" pattern (Wormser *et al.* 2006). The first tier is an

enzyme-linked immunosorbent assay (ELISA). If a positive ELISA test result is

obtained, then the second tier for confirmation is a Western blot for immunoglobulin M

(IgM) or immunoglobulin G (IgG) (Sanchez *et al.* 2016). As the antibody response to *B.*

burgdorferi develops slowly, diagnostic testing at the early stages of infection may yield

negative results (Depietropaolo *et al.* 2005). If infection with *B. burgdorferi* remains a

suspected cause, tests need to be repeated two to four weeks later (Depietropaolo *et al.*

2005). Testing for IgM or IgG is dependent on the length of time for which the

symptoms persisted; if symptoms have persisted for four weeks or longer, an IgG

immunoblot should be performed as the IgM antibody response begins to decline

(Steere *et al.* 2004). Early during infection, IgM immunoblots are more useful as these

antibodies are made first in response to infection (Wormser *et al.* 2006); however, as

infection progresses, the antibody response switches to IgG (Steere *et al.* 2004). Use

of IgM immunoblots for diagnosis in later stages of infection may yield false positive

results due to presence of cross-reactive antibodies (Steere *et al.* 2004), demonstrating

the need for more specific diagnostic tests.

Oral antibiotics, such as doxycycline or amoxicillin, are recommended for patients who

have been diagnosed with Lyme disease early during the course of infection (Wormser

et al. 2006). For those suffering from symptoms of disseminated infection, intravenous

administration of ceftriaxone is recommended (Wormser *et al.* 2006). If treated early

during infection, most patients suffer no lasting effects from disease. However, a lack of

diagnosis or misdiagnosis of symptoms, particularly those exhibited during the early

localized stage of infection, may lead to lack of treatment or administration of

inadequate medications. Additionally, despite proper antibiotic treatment, a small subset of individuals may continue to suffer from persistent symptoms.

Immunology of Lyme Arthritis

One of the common manifestations associated with the late-persistent stage of infection is Lyme arthritis, which affects approximately 60% of infected individuals (Steere and Glickstein 2004). Lyme arthritis is characterized by intermittent episodes of inflammation in large joints, particularly the knee, followed by periods of remission. Severe cases may result in cartilage and bone erosion, leading to permanent loss of joint function (Steere *et al.* 2004). Upon infection with *B. burgdorferi*, the immune system attempts to eliminate the bacteria, inducing a robust inflammatory response which leads to clinical manifestations of disease. An unregulated inflammatory response can lead to tissue damage consistent with the early disseminated and late persistent stages of infection. Different subsets of adaptive immune cells have been implicated in disease pathogenesis, particularly T helper type 1 (Th1) cells and T helper type 17 (Th17) cells. A third subset of T helper cells, T helper type 2 (Th2) cells, has been implicated in disease resolution.

Th1 cells are a type of immune cell responsible for the promotion of inflammation and are believed to contribute to the development of arthritis following infection with *B. burgdorferi*. Elevated numbers of Th1 cells have been found in the joint fluid of patients with Lyme arthritis (Gross *et al.* 1998), suggesting a role for these cells in development of disease. Murine studies have demonstrated that interferon-gamma (IFN-γ), a pro-inflammatory cytokine secreted by Th1 cells, contributes to disease pathogenesis (Kang

et al. 1997). However, subsequent studies have demonstrated that Lyme arthritis can be induced in the absence of IFN-γ (Brown and Reiner 1999), suggesting that additional immune cells promote inflammation in Lyme arthritis.

Another pro-inflammatory cytokine, interleukin-17 (IL-17), is a possible additional mediator of Lyme arthritis. Studies in a mouse model of severe Lyme arthritis demonstrated that administration of anti-IL-17 antibodies prevented the development of disease (Burchill *et al.* 2003). This finding implicated IL-17 as another contributor to the development of Lyme arthritis. IL-17 is the primary cytokine produced by Th17 cells, suggesting Th17 cells may also be involved in arthritis development. Further support for this conclusion was provided upon analysis of interleukin-23 (IL-23), a cytokine crucial for the survival of Th17 cells. Blocking of IL-23 with anti-IL-23 antibodies prevented the development of arthritis in mice and decreased the amount of IL-17 produced to contribute to arthritis development (Kotloski *et al.* 2008).

Studies of human patients have suggested that Th17 cells are also involved in the development of Lyme arthritis. These cells can be induced by the *B. burgdorferi* neutrophil-activating protein A (NapA). NapA-specific Th17 cells were found to contribute to inflammation by secretion of IL-17, which led to bone destruction (Codolo *et al.* 2008). Recently, it has been found that elevated levels of IL-23 were present in a subset of individuals with an erythema migrans rash who suffered from arthritis following antibiotic administration (Strle *et al.* 2014). This also suggests that Th17 responses contribute to disease pathology.

Conversely, the presence of Th2 cells is correlated with a faster resolution of Lyme arthritis. Accumulation of Th2 cells in the joint fluid of patients with Lyme arthritis was found to be correlated with the down-regulation of Th1 cells (Gross *et al.* 1998). This increase in Th2 cell numbers led to a shorter duration and decreased severity of arthritis (Gross *et al.* 1998). Higher numbers of Th2 cells may correlate with production of increased levels of their characteristic cytokine, interleukin-4 (IL-4). Further support for the role of Th2 cells in disease was provided by a study in BALB/c mice, which demonstrated that high levels of IL-4 correlated with decreased arthritis severity following infection with *B. burgdorferi* and that blocking of IL-4 resulted in more severe arthritis (Matyniak and Reiner 1995). However, further studies demonstrated that IL-4 was not necessary for resistance to development of arthritis but may instead play a role in the stimulation of an effective immune response against *B. burgdorferi* (Brown and Reiner 1999).

Antibiotic-Refractory Lyme Arthritis

Antibiotic therapy is usually sufficient to resolve arthritis; however, symptoms persist in 10% of patients (Steere and Glickstein 2004). This persistence of arthritic symptoms despite appropriate antimicrobial treatment is termed antibiotic-refractory Lyme arthritis. Antibiotic-refractory Lyme arthritis is defined as persistent inflammation of the joint for at least two months following completion of a course of antibiotics (Stanek *et al.* 2011). The precise explanation for why this small subset of patients continues to suffer from lasting effects of disease has not been elucidated; however, a variety of plausible mechanisms have been proposed. Two such mechanisms include induction of an autoimmune response or the persistence of spirochetal antigens within the joint tissue.

Major histocompatibility complex class II human leukocyte antigen (HLA)-DR4-mediated presentation of autoantigens is believed to contribute to the development of antibiotic-refractory Lyme arthritis (Steere and Glickstein 2004). Recently, it was found that endothelial cell growth factor (ECGF), a chemotactic factor that stimulates proliferation of endothelial cells and also induces angiogenesis, was elevated in the joint fluid and tissue of patients with antibiotic-refractory Lyme arthritis (Drouin *et al*. 2013). B and T cell responses to ECGF were found to occur in these patients (Drouin *et al*. 2013), suggesting an autoimmune mechanism in the development of antibiotic-refractory Lyme arthritis.

Analysis of synovial fluid (Nocton *et al*. 1994) and synovial tissue samples (Carlson *et al*. 1999) from patients with antibiotic-refractory Lyme arthritis by polymerase chain reaction (PCR) for probes specific to *B. burgdorferi* outer surface proteins did not reveal the presence of viable spirochetes. Thus, the persistent symptoms in these patients were not believed to be due to chronic infection. A study in mice treated with doxycycline demonstrated that *B. burgdorferi* antigens persisted in cartilage and joint surfaces for extended periods of time following treatment (Bockenstedt *et al*. 2012). This finding suggests that antibiotics eliminate infectious bacteria from the host, but antigenic fragments may not be effectively cleared. In addition, Wormser *et al*. proposed the "amber theory", which suggests that dead *B. burgdorferi* spirochetes, and their antigenic fragments, can be found in the connective tissue of infected patients (Wormser *et al*. 2012). When alive, these microorganisms attach to, and colonize, joint tissue, and may remain attached following their death after antimicrobial therapy.

These confined microorganisms and their fragments may gradually be released into the joint space over time, eliciting an inflammatory response (Wormser *et al.* 2012). Peptidoglycan, a major component of the bacterial cell wall, has recently been identified as a potential persistent antigen contributing to the pathogenesis of Lyme arthritis, with peptidoglycan unique to *B. burgdorferi* being detected in 94% of synovial fluid samples taken from numerous patients with antibiotic-refractory Lyme arthritis (Jutras *et al.* 2019). These dead spirochetes and antigenic fragments may still stimulate an immune response but will not yield a positive PCR result.

Murine Models of Lyme Disease

Researchers utilize mouse models to investigate the pathogenesis of Lyme disease. Some aspects of disease, particularly carditis and arthritis, resemble those seen in humans following infection with *B. burgdorferi*. Studies of Lyme borreliosis in mice revealed that spirochetes disseminate to the spleen and through the blood to distant tissues such as the heart and joints within a few days after inoculation into the skin, and subsequently induce inflammation in these tissues (Barthold *et al.* 1991). Disease manifestations correlated with the appearance of spirochetes within these target tissues, and it was determined that the immune responses to infection in mice were characteristic of those seen in humans (Barthold *et al.* 1991). It has been established that mouse strains of differing genetic backgrounds vary in their response to infection with *B. burgdorferi*. For example, C3H mice have been shown to develop severe arthritis following infection. BALB/c mice have been shown to develop carditis, and, in the case of arthritis, a greater number of joints were involved than that seen in C3H mice; however, disease severity is decreased in these mice (Barthold *et al.* 1990). By

contrast, C57BL/6 mice tend to exhibit minimal or mild symptoms of carditis or arthritis (Barthold *et al*. 1990). Additionally, the disease manifestations associated with varied doses of *B. burgdorferi* differ among mouse strains. C57BL/6 mice are resistant to arthritis development at a variety of doses of *B. burgdorferi*, ranging from $2x10^2$ to $2x10^5$ organisms (Ma *et al*. 1998). In contrast, BALB/c mice exhibit a dose-dependent response to *B. burgdorferi* infection, as infection with higher doses of bacteria correlated with greater arthritis severity, while infection with lower doses of bacteria correlated with little to no arthritis (Ma *et al*. 1998).

Immunological differences may explain differences in clinical manifestations between mouse strains. When compared to the highly Lyme disease-susceptible C3H mice, BALB/c mice tend to be more resistant to disease. Early during infection, BALB/c mice develop a Th1 response, as evidenced by elevated levels of IFN-γ and IL-2 (Zeidner *et al*. 1997). Further studies demonstrated that both C3H and BALB/c mice produced higher levels of IFN-γ early in Lyme arthritis (Kang *et al*. 1997), indicating that the initial development of Lyme arthritis is mediated by a Th1 response. However, two weeks after infection, an elevated level of IL-4 was observed only in BALB/c mice, and this correlated with decreased arthritis severity in this strain (Kang *et al*. 1997). This indicates that the decreased arthritis severity seen in BALB/c mice was likely mediated by a Th2 response. As the BALB/c mice tend to be naturally biased towards developing a Th2 response, this may explain the difference in disease severity between BALB/c and C3H mice. Taken together, these findings suggest that the Th2 response in BALB/c mice, although not protective, may contribute to a faster resolution of Lyme arthritis than that seen in C3H mice. Differences in disease severity are also observed

between BALB/c mice and C57BL/6 mice, with C57BL/6 mice being more resistant to the development of arthritis, which could also be attributed to immunological differences between these two mouse strains.

Regulatory T Cells

Regulatory T (Treg) cells are a population of T cells responsible for control of the immune response. Treg cells have been implicated in preventing graft vs. host disease. Additionally, immune dysregulation, possibly due to non-functional Treg cells, has been linked to development of autoimmune diseases such as diabetes, thyroiditis, inflammatory bowel diseases, and rheumatoid arthritis (Brusko *et al*. 2008). Treg cells were previously characterized by their expression of CD4, and high levels of CD25, but are now distinguished by their expression of Foxp3 (forkhead box P3). Foxp3 is a transcription factor that is critical for the development of Treg cells. It is regarded as a molecular marker unique to Treg cells (Fontenot *et al*. 2003), making this important for distinguishing Treg cells from other populations of immune cells.

Differentiation of naïve T cells into Treg cells is stimulated by transforming growth factor beta (TGF-β), which is a cytokine that has varying effects depending on the environmental context (Sanjabi *et al*. 2009). TGF-β, in the presence interleukin 6 (IL-6), leads to the production of Th17 cells, whereas TGF-β alone stimulates development of Treg cells (Bettelli *et al.* 2006). Additionally, TGF-β signaling has been found to be responsible for Foxp3 induction in the development of natural Treg cells, as deletion of the TGF-β receptor blocked their development (Liu *et al*. 2008).

The development of "depletion of regulatory T cell", or DEREG, mice, has enabled researchers to study the effects of Treg cells in various diseases. DEREG mice have been engineered to express a fusion protein comprised of a diphtheria toxin (DTx) receptor and an enhanced green fluorescent protein. This protein is under the control of the foxp3 promoter (Lahl *et al.* 2007). As Foxp3 is regarded as the definitive marker for identification of Treg cells (Fontenot *et al.* 2003), this mouse model allows for the selective depletion of Treg cells via administration of small amounts of diphtheria toxin (DTx). With two consecutive days of injection with 1 μg of DTx (Lahl and Sparwasser 2011), 95% to 98% of Foxp3$^+$ Treg cells are depleted (Lahl *et al.* 2007).

Role of Regulatory T Cells in Lyme Disease

Studies in mice have implicated a role for CD4+CD25+ putative Treg cells in experimental Lyme arthritis. In IFN-γ-deficient mice primed and infected with *Borrelia* species, treatment with anti-IL-17 antibody prevented disease and resulted in an increase in the numbers of CD4+CD25+ T cells (Nardelli *et al.* 2004). Administration of anti-CD25 antibodies at the time of IL-17 neutralization decreased the numbers of CD4+CD25+ T cells and caused these mice to develop severe arthritis (Nardelli *et al.* 2004). In addition, adoptive transfer of CD4+CD25+ T cells obtained from IFN-γ-deficient mice treated with anti-IL-17 antibody prevented the development of arthritis (Nardelli *et al.* 2005). However, in *B. burgdorferi*-infected IFN-γ-deficient mice in which IL-17 was not blocked, administration of anti-CD25 antibody did not have a significant effect on arthritis (Nardelli *et al.* 2006). This suggested a role for putative CD4+CD25+ Treg cells in the prevention of Lyme arthritis, and that their development was linked to IL-17. This was supported by the findings of Bettelli *et al.*, in which a cytokine-

14

dependent, inverse relationship between the development of Th17 cells and Treg cells was demonstrated. The "anti-inflammatory" environment found in the animals treated with anti-IL-17 antibody likely led to the development of Treg cells, whereas the IL-17-driven inflammation in the untreated animals did not lead to development of Treg cells. Together, these findings provided initial support for the conclusion that symptoms of Lyme disease may occur as a result of lower numbers of Treg cells.

Additionally, a role for Treg cells in the control of human Lyme arthritis has been suggested. It was shown that higher numbers of Treg cells in the joint fluid of patients with antibiotic-resistant Lyme arthritis correlate with a faster eventual resolution of arthritis (Shen *et al.* 2010). In addition, it has been shown that patients with antibiotic-refractory disease have lower numbers of Treg cells than patients who respond to antibiotics (Vudattu *et al.* 2013). These findings support a possible role for Treg cells in the control of arthritis development in patients with antibiotic-refractory Lyme arthritis.

More recent studies have demonstrated that specific depletion of Treg cells prior to infection with *B. burgdorferi* caused the development of arthritis in DEREG mice of the otherwise arthritis-resistant C57BL/6 mouse strain (Nardelli *et al.* unpublished data). In addition, depletion of Treg cells after infection of these mice resulted in an increase in swelling of the hind paws. These findings provide more direct support for a role for Treg cells in the control of Lyme arthritis. However, while the results of these experiments demonstrated a role for Treg cells in a model of resistance to Lyme disease, the role of Treg cells has not been studied in the context of disease, as would occur in susceptible mouse strains.

II. Hypothesis and Specific Aims

Lyme disease is a multi-stage disease that affects multiple organ systems of the body. Clinical manifestations of disease result from the inflammatory response elicited to aid in clearance of the pathogen. Treg cells are a subset of cells responsible for controlling the immune system (Sakaguchi *et al.* 2008). While previous studies have demonstrated a possible role for Treg cells in controlling the development of Lyme arthritis, the role of Treg cells has not been studied directly in the context of Lyme disease to a great extent. Additionally, little evidence exists as to the role of Treg cells in the control of the immune response to disseminated infection with *B. burgdorferi*. The overall objective of this thesis is to determine the role of Treg cells in the development and progression of Lyme disease in a disease-susceptible mouse model.

The central hypothesis of this thesis is that Treg cells control the development and progression of Lyme disease following *B. burgdorferi* infection. To test this hypothesis, two specific aims were addressed. The first specific aim was to determine the effect of Treg cells on the development of arthritis following infection with *B. burgdorferi*. The working hypothesis of this specific aim was that depletion of Treg cells will exacerbate tibiotarsal joint swelling and arthritis following *B. burgdorferi* infection. The second specific aim was to determine the effect of Treg cells on the control of the immune response following infection with *B. burgdorferi*, with the working hypothesis that depletion of Treg cells would result in an increased ability to control bacterial dissemination and increased levels of pro-inflammatory cytokines following *B. burgdorferi* infection.

CHAPTER 2: MATERIALS AND METHODS

Mice: Preliminary experiments were conducted using four-week-old wild-type (WT) BALB/c mice purchased from The Jackson Laboratory (Bar Harbor, ME). These WT mice were allowed to acclimate to the new housing facility and were used for experiments beginning at six weeks of age. All studies were completed using six-to-eight-week-old WT mice and "depletion of regulatory T cell," or DEREG, mice on the BALB/c background. BALB/c DEREG mice were bred in-house. Mice were housed at the University of Wisconsin-Milwaukee Animal Research Center in a humidity-controlled environment at a temperature of 21°C with a regulated 12-hour light and dark cycle. Food and acidified water were provided *ad libitum*. All protocols were reviewed and approved by the University of Wisconsin-Milwaukee Institutional Animal Care and Use Committee (IACUC).

Group Assignment: For preliminary experiments, WT BALB/c mice were randomly assigned to groups which consisted of mice infected with either $2X10^3$, $2X10^4$, or $2X10^5$ organisms (described below). Mice administered the vehicle, phosphate buffered saline (PBS) supplemented with heat-inactivated normal mouse serum (NMS) comprised an uninfected control group. For all subsequent studies (described below), both WT and DEREG mice were randomly assigned to groups. Some groups of BALB/c WT and BALB/c DEREG mice were administered diphtheria toxin (DTx) in PBS prior to infection with *B. burgdorferi*. In addition, groups of BALB/c DEREG mice were administered PBS alone prior to infection with *B. burgdorferi*. Additional groups consisted of BALB/c DEREG mice administered DTx in PBS prior to injection with PBS supplemented with

NMS and BALB/c DEREG mice administered PBS alone prior to injection with PBS supplemented with NMS. All groups consisted of three to eight mice.

Genotyping: Genotyping of pups was performed according to protocols developed by The Jackson Laboratory (Bar Harbor, ME) using a tail sample obtained at the time of weaning. DNA was extracted from the tail samples by adding 75 µL of a digestion buffer consisting of 25 mM NaOH and 0.2 mM EDTA, and boiling for one hour at 98°C. Samples were then cooled to room temperature, and 75 µL of 40 mM Tris HCl pH of 5.5 was added to each sample. Samples were centrifuged at 4,000 rpm for three minutes and then used for polymerase chain reaction (PCR) amplification. Forward and reverse primer sequences used for characterization of WT mice were 5'-CAAATGTTGCTTGTCTGGTG-3' and 5'-GTCAGTCGAGTGCACAGTTT-3', respectively (Eurofins Genomic, Louisville, KY). Forward and reverse primer sequences for the transgene were 5'-CCCAGGTTACCATGGAGAGA-3' and 5'-GAACTTCAGGGTCAGCTTGC-3', respectively (Eurofins Genomic, Louisville, KY). WT and transgene primers were used in separate PCR reactions, which were prepared by adding 12.0 µL of Denville Hot Start Mastermix, 0.8 µM of each forward and reverse primers, 5.0 µL of PCR grade water, and 4.0 µL of DNA, for a 25 µL total reaction volume. The PCR amplification protocol consisted of an initial denaturation step at 94°C for two minutes, followed by 35 cycles of denaturation at 94°C for 45 seconds, annealing at 60°C for 30 seconds, and extension at 72°C for two minutes, followed by a final extension step at 72°C for ten minutes, and a final hold step at 4°C. Amplified DNA products were run on a 1.5% weight per volume (w/v) agarose gel containing ethidium bromide at 135-140 volts for one hour and were imaged under ultraviolet light. DEREG

mice were identified by the presence of the transgene, which was confirmed by the appearance of a 380 base pair sized band on the gel.

Depletion of Treg Cells: Lyophilized diphtheria toxin (DTx) from *Corynebacterium diphtheriae* (Calbiochem, San Diego, CA; Fisher Scientific, Lenexa, KS) was reconstituted in filter-sterilized PBS, aliquoted, and then stored at -80°C until use. Diphtheria toxin was diluted from stock solutions into filter-sterilized PBS to a final concentration of 0.02 µg/mL. Fifty µL (1 µg) of DTx in PBS, or PBS alone, was injected intraperitoneally into the mice for two consecutive days prior to infection with *B. burgdorferi* (Day -2 and Day -1, respectively). Previous studies have demonstrated that 1 µg of DTx, administered on two consecutive days, was sufficient for depleting Treg cells for approximately five days following administration (Lahl and Sparwasser 2011). Mice were anesthetized prior to all injections with a 20% volume per volume (v/v) mixture of isoflurane in propylene glycol. Weight loss is a common side effect following administration of DTx (Mayer *et al.* 2014). To monitor for any potential morbidity associated with DTx administration, mice were weighed immediately prior to administration of DTx and then every day following injection until the mice began exhibiting consistent weight gain, at which time mice were weighed every four days until euthanasia.

Flow Cytometry: In a preliminary experiment, spleens were collected on the day immediately following administration of a second dose of DTx in order to assess the efficacy of DTx in depleting Treg cells. A single cell suspension of splenocytes was prepared by teasing apart the spleens and passing the cells through a 0.2 µm sterile

nylon mesh filter into cold Dulbecco Modified Eagle's Medium (DMEM). Splenocytes were then enumerated using a hemocytometer and placed into chilled flow tubes. The eBioscience Mouse Regulatory T Cell Staining Kit (Thermo Fisher Scientific, Waltham, MA) was used for flow cytometric analysis of Treg cells following the manufacturer's protocols. Cells were incubated with 1.5 µL of both fluorescein isothiocyanate (FITC)-labeled anti-CD4 antibodies and phycoerythrin (PE)-labeled anti-CD25 antibodies. Cells were fixed and permeabilized and then incubated with 1.5 µL of allophycocyanin (APC)-labeled anti-Foxp3 antibodies. Compensation controls consisted of both single-stained and double-stained populations for all possible antibody combinations, with isotype control antibodies being used as unstained controls. Data were acquired using a BD FACSAria flow cytometer using FlowJo software (BD Biosciences, San Jose, CA). Events were gated to include all lymphocytes, with ten thousand events being collected and analyzed using a dot plot.

Bacterial Preparation and Infection: _Borrelia burgdorferi_ strain B31-A3 organisms grown in modified Barbour-Stoenner-Kelly (BSK) medium were generously provided by Dr. Jenifer Coburn (Medical College of Wisconsin) and were frozen at -80°C until use. Low passage (<10) organisms were grown by adding 10 µL of stock culture to 4 mL of BSK medium with or without the presence of 2.5 µg/mL Amphotericin B, 20 µg/mL Fosfomycin, and 50 µg/mL Rifampin (Curtis _et al_. 2018) and incubated at 34°C. Growth and motility of _B. burgdorferi_ were visualized using dark-field microscopy.

On the day of infection, microbes were washed twice in PBS supplemented with NMS. Microbes were resuspended in PBS supplemented with NMS and were visualized by

dark field microscopy for motility. Viable organisms were enumerated using a Petroff-Hausser counting chamber. Spirochetes were then diluted to different concentrations depending upon the infectious dose to be used for experiments. Mice were anesthetized with a 20% v/v mixture of isoflurane in propylene glycol and then injected subcutaneously between the scapulae with $1X10^2$, $1X10^3$, $2X10^3$, $2X10^4$, or $2X10^5$ organisms in 20 µL of PBS supplemented with NMS. Non-infected control groups consisted of mice injected with PBS supplemented with NMS.

Assessment of Tibiotarsal Joint Swelling: Edematous changes in the tibiotarsal joints of mice were assessed in order to provide a measure of inflammation associated with *B. burgdorferi* infection. Mice were anesthetized with a 20% v/v mixture of isoflurane in propylene glycol. A digital caliper (Marathon) was used to measure the width and thickness of the tibiotarsal joint. The width and thickness measurements were then averaged to provide a mean caliper reading. For preliminary experiments, baseline measurements were obtained prior to infection (Day 0) and then tibiotarsal joints were measured every seven days following infection for a total of 35 days. In one study, baseline measurements were obtained the day following administration of diphtheria toxin just prior to infection with *B. burgdorferi*, and joints were measured every four days following infection for a period of 20 days. In another study, baseline measurements were obtained, and joints were measured every four days following infection for a period of 35 days. Changes in tibiotarsal joint swelling were determined by calculating the difference from baseline measurements.

Pathological Assessment of Arthritis: Hind paws were amputated above the knee joint, and one hind paw from each mouse was fixed in 10% buffered formalin. Blinded histopathological analysis was performed by a board-certified pathologist (Dr. Michael Lawlor, Medical College of Wisconsin). Pathology of the hind paws was scored on a scale of 0-3 based on the degree of leukocytic infiltration, hyperplasia, and cartilage and bone erosion. A score of 0 indicated absence of pathology; a score of 1 indicated a single small focus of inflammation; a score of 2 indicated two or three small foci of inflammation; and a score of 3 indicated several larger areas of inflammation.

Quantification of Bacterial Load in Mouse Tissue: The remaining hind paw and a bisected portion of the hearts were flash frozen in liquid nitrogen and then stored at -80°C to be used for quantitative polymerase chain reaction (qPCR) analysis of bacterial load in these tissues. DNA was extracted from these tissues using the Qiagen DNeasy Mini Kit (Qiagen, Germantown, MD) following the manufacturer's protocol. Extracted DNA was quantified using a NanoDrop One (Thermo Scientific, Waltham, MA). Bacterial load was assessed using a Synergy Brands, Inc. (SYBR) green-based qPCR technique described by Ristow *et al.* (2012). Primers for the *B. burgdorferi* chromosomal gene *recA* were used [(forward: 5-GCAGCTATCCCACCTTCTTT-3'); (reverse: 5'-ATGAGGCTCTCGGCATTG-3')]. Values were normalized based on copies of *Mus musculus β-actin* [(forward: 5'-TCACCCACACTGTGCCCATCTACGA-3'); (reverse: 5'-GGATGCCACAGGATTCCATACCCA-3')]. Standard curves for bacterial and mouse targets were obtained and used as the basis for quantification of bacterial load within tissue samples. Separate reaction mixtures were prepared for each primer set, with the reaction mixture consisting of 10 μL of PowerUp SYBR Green Master Mix

(Life Technologies, Carlsbad, CA), 0.5 µM of both forward and reverse primers for either gene, 1 µL of PCR grade water, 2.5 mM MgCl$_2$, and 5 µL of DNA. The amplification protocol consisted of a pre-cycling step at 50°C for two minutes and an initial denaturation step at 95°C for two minutes, followed by 40 cycles of denaturation at 95°C for 15 seconds and annealing at 60°C for one minute. A melt curve analysis protocol consisted of 15 seconds at 95°C, one minute at 60°C, then gradually heating to 95°C for 15 seconds. Analyses were performed using an Applied Biosystems StepOnePlus^{TM} Real-Time PCR System (Applied Biosystems, Waltham, MA). *B. burgdorferi recA* gene copies were normalized to mouse *β-actin* after being calculated from standard curves.

Analysis of Serum Cytokines: Blood was collected at the time of euthanasia by intracardiac puncture and sera were obtained and stored at -80°C until use. A Mouse Magnetic Luminex Assay Kit (R&D Systems, Minneapolis, MN) was used to determine the levels of serum cytokines associated with pro- and anti-inflammatory immune responses. Cytokines assayed included granulocyte-macrophage colony-stimulating factor (GM-CSF), IFN-γ, IL-1β, IL-2, IL-4, IL-5, IL-6, IL-10, IL-12 p70, IL-13, IL-17A, and tumor necrosis factor alpha (TNF-α). Serum samples were diluted and a standard curve was created according to the manufacturer's protocol. A negative assay control consisting of calibrator diluent was used to determine the background fluorescence levels. Serum samples were analyzed on a Magpix instrument with xPONENT software (R&D Systems, Minneapolis, MN). Cytokine levels were calculated for each analyte using the respective standard curve. All samples were run in triplicate, and the values were averaged to provide a mean cytokine level for each respective sample.

Statistics: Data were analyzed using GraphPad Prism Version 8.2 (GraphPad Software, San Diego, CA). It was reasoned, *a priori*, that *B. burgdorferi*-infected mice depleted of Treg cells would exhibit greater signs of inflammation than would infected mice not depleted of Treg cells. The Mann-Whitney U Test (GraphPad Prism) was used to analyze differences in tibiotarsal joint swelling, arthritis scores, borrelial load, and cytokine concentrations between infected BALB/c DEREG mice previously administered DTx or not administered DTx, as well as between infected BALB/c DEREG and BALB/c WT mice that were previously administered DTx. The alpha level was set at 0.05 prior to initiation of experiments. Data were expressed as mean ± standard error of the mean (SEM) unless otherwise stated.

CHAPTER 3: RESULTS

I. Preliminary Studies

Dose-dependent response to infection with B. burgdorferi *in WT BALB/c mice.* The

purpose of this experiment was to determine an infectious dose of *B. burgdorferi*

sufficient to induce moderate disease in BALB/c mice, such that any potential

pathological effects of Treg cell depletion in these mice could be observed. It has been

reported that BALB/c mice exhibit tibiotarsal joint swelling in a dose-dependent manner

when infected with *B. burgdorferi* (Ma *et al.* 1998). Mice were injected subcutaneously

between the scapulae with $2X10^3$, $2X10^4$, or $2X10^5$ *B. burgdorferi* organisms in PBS

supplemented with NMS or with PBS supplemented with NMS alone. No swelling was

observed for the first week following infection in mice infected with $2X10^3$ and $2X10^4$

spirochetes, after which time joint swelling steadily increased. Mice infected with $2X10^3$

organisms exhibited a milder degree of tibiotarsal joint swelling (Figure 1), than mice

infected with $2X10^4$ organisms. By contrast, slight tibiotarsal joint swelling was

observed within the first week in mice infected with $2X10^5$ organisms. Joint swelling

continued to increase for the duration of the experiment, ending with a degree of

tibiotarsal joint swelling higher than mice infected with either $2X10^3$ or $2X10^4$ organisms.

No changes in tibiotarsal joint swelling was observed in uninfected mice. No statistically

significant differences were observed between mice infected with the different doses of

B. burgdorferi. However, significant differences in joint swelling were observed between

uninfected mice and mice infected with both $2X10^4$ and $2X10^5$ organisms beginning at

Day 21 and continuing for the duration of the experiment. Based on these results, it

was determined that an infectious dose of not more than $2X10^3$ organisms would be

used to assess the effects of Treg cells on the development and progression of Lyme

disease as Treg cell depletion is expected to worsen disease.
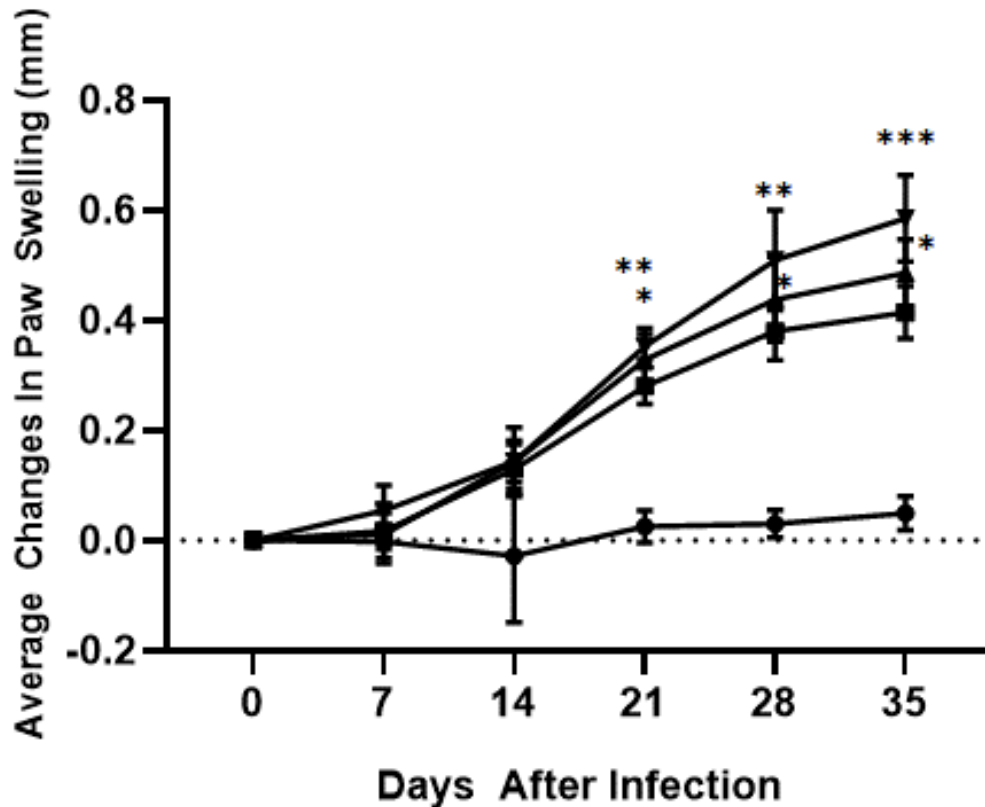
Figure 1: Average changes in tibiotarsal joint swelling in response to infection with increasing doses of *B. burgdorferi*. BALB/c WT mice were infected with either PBS + NMS (n=7) (circles) or, $2X10^3$ (n=4) (squares), $2X10^4$ (n=6) (triangles), or $2X10^5$ (n=6) (cones) spirochetes. Error bars represent SEM. * $P \le 0.05$. ** $P \le 0.01$. *** $P \le 0.001$. Asterisks denote statistically significant differences when compared to uninfected BALB/c WT mice.

Effect of DTx on Treg cell depletion in DEREG mice. Previous studies have

demonstrated that 1 µg of DTx administered for two consecutive days was sufficient for

the rapid depletion of Treg cells (Lahl and Sparwasser 2011). Two different lots of

diphtheria toxin were used for these studies, so it was necessary to compare the activity

of each lot of diphtheria toxin to confirm that their depletion efficiencies were similar. In

PBS control mice, 2.61% of lymphocytes expressed Foxp3 (Table 1). As expected, the

average percentage of splenic lymphocytes that were positive for Foxp3 was

decreased, but the decrease was similar between mice administered the two lots of

diphtheria toxin, with 0.66% and 0.53% of lymphocytes positive for Foxp3, respectively.

When compared to the average percentage of Foxp3+ cells from mice administered

PBS alone, DTx reduced the average percentages of Foxp3$^+$ lymphocytes by

approximately 75% and 80%, respectively.

Table 1: Toxin effectiveness as determined by flow cytometric detection of Treg cell percentages. Data represent average percentage of splenic lymphocytes that were positive for Foxp3 ± SEM. N=3

Group	% Foxp3+
PBS	2.61 ± 0.01
Lot 1 of DTx	0.66 ± 0.26
Lot 2 of DTx	0.53 ± 0.18

II. Specific Aim 1: Determine the effect of Treg cells on the development of arthritis following *B. burgdorferi* infection.

Effect of diphtheria toxin (DTx) on weight in treated mice. Mice were weighed to monitor

potential health effects following diphtheria toxin administration. For one study, the

effects of DTx on mouse weight were determined in mice infected with 1X10^2 *B.*

burgdorferi organisms. BALB/c DEREG mice administered PBS, without DTx, and

infected with *B. burgdorferi* exhibited consistent weight gain for the duration of the 20-

day experiment (Figure 2). Additionally, no weight loss was observed in BALB/c

DEREG mice administered DTx prior to infection with *B. burgdorferi*. However, there

was no steady increase in weight in these mice from days -2 to 5 after infection. Following this, a slight increase in weight occurred from days 5 to 8 after infection, at which time the weights remained steady but lower than in infected mice not previously administered DTx. While changes of weight in BALB/c DEREG mice administered DTx prior to infection were less than in BALB/c DEREG mice administered PBS prior to infection, they were not statistically significant. By contrast, an initial weight loss was observed on the first day following infection in *B. burgdorferi*-infected BALB/c WT mice previously administered DTx, with weight decreasing slightly over the next three days. On day 5 following infection and subsequently thereafter, the mice began to steadily gain weight. This weight gain was comparable to that observed in BALB/c DEREG mice administered PBS prior to infection with *B. burgdorferi*. These weight changes were greater in BALB/c WT mice administered DTx prior to infection than in BALB/c DEREG mice administered DTx prior to infection; however, these differences were not statistically significant. Uninfected BALB/c DEREG mice previously administered DTx exhibited no weight gain for the first three days following infection. The mice then gained a modest amount of weight beginning four days after infection, with the weight remaining relatively unchanged from day twelve and onward following infection.
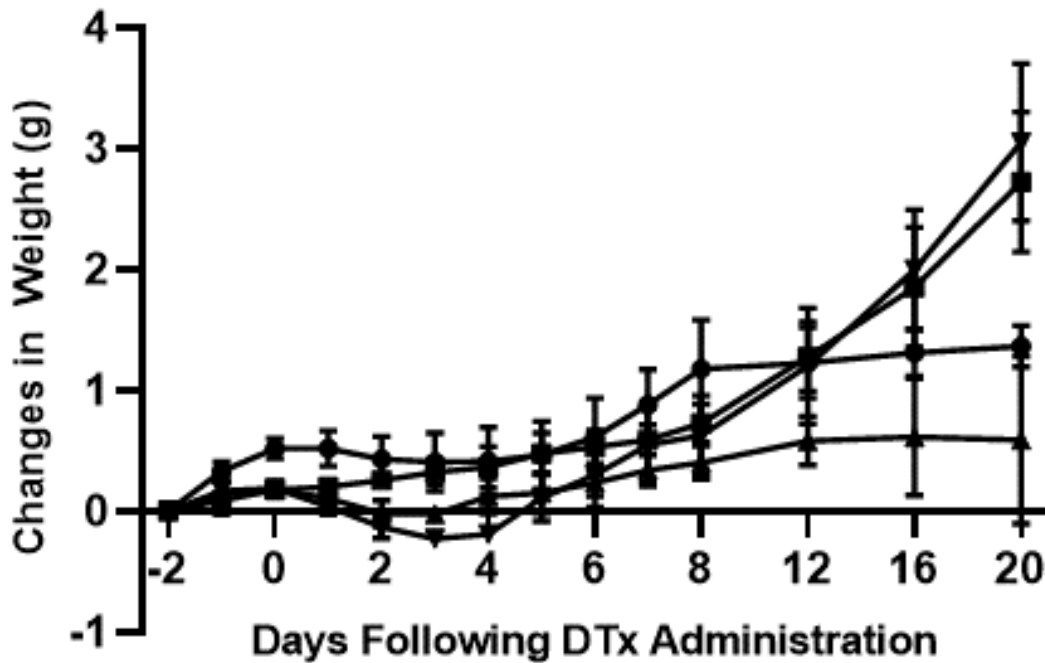
Figure 2. Average changes in weight following administration of diphtheria toxin in mice infected with 1X10^2 *B. burgdorferi*. Groups consisted of BALB/c DEREG mice administered DTx prior to infection with *B. burgdorferi* (n=4) (circles); *B. burgdorferi*-infected BALB/c DEREG mice not previously administered DTx (n=4) (squares); uninfected BALB/c DEREG mice previously administered DTx (n=3) (triangles); and BALB/c WT mice administered DTx prior to infection with *B. burgdorferi* (n=4) (cones). Error bars represent SEM.

In another study, the effects of DTx on weight were determined in mice infected with 1X10^3 *B. burgdorferi* organisms. BALB/c DEREG mice that were administered PBS prior to infection with *B. burgdorferi* exhibited consistent weight gain throughout the course of the 35-day experiment (Figure 3). By contrast, in BALB/c DEREG mice administered DTx prior to infection with *B. burgdorferi*, a delay in weight gain was observed for the first three days following infection. From day 3 until day 11 following infection, the mice began to exhibit a slight weight gain. A weight loss was observed from day 11 until day 16, although the changes in weight remained above baseline. From day 16 until the end of the experiment, these mice exhibited consistent weight

gain. Although weights in these mice were lower than those observed for BALB/c DEREG mice administered PBS prior to infection, the differences were not statistically significant. In addition, BALB/c WT mice administered DTx prior to infection with *B. burgdorferi* exhibited a relatively consistent weight gain for the duration of the experiment, much like the weight gain observed in infected BALB/c DEREG mice previously administered PBS. The weights observed in BALB/ WT mice administered DTx prior to infection were greater than those observed in BALB/c DEREG mice administered DTx prior to infection; however, no statistically significant differences were observed. By contrast, in uninfected BALB/c DEREG mice administered DTx, an initial weight loss for the first two days following DTx administration was observed. After the initial weight loss, the weight returned to baseline levels and remained unchanged until day 12 after infection. At this point, the weight began to increase for the remainder of the experiment. Finally, uninfected BALB/c DEREG mice administered PBS exhibited consistent weight gain for the duration of the experiment.
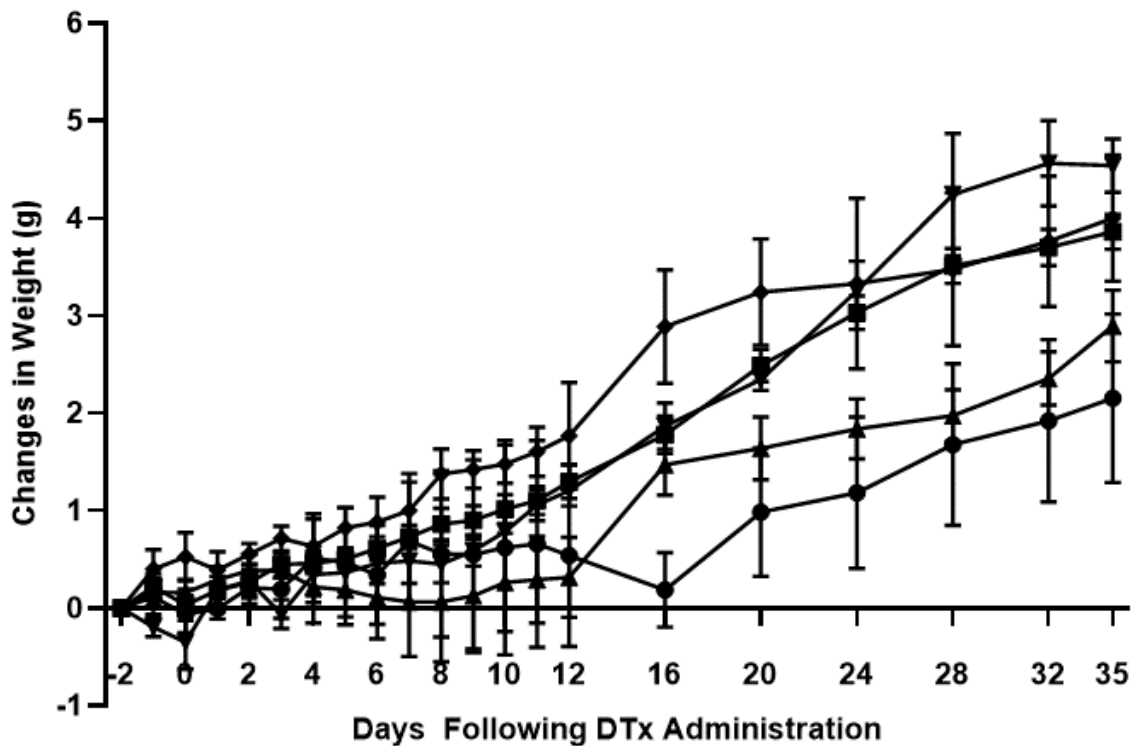
Figure 3: Average changes in weight following administration of diphtheria toxin in mice infected with 1X10^3 *B. burgdorferi*. Groups consisted of BALB/c DEREG mice administered DTx prior to infection with *B. burgdorferi* (n=7) (circles); *B. burgdorferi*-infected BALB/c DEREG mice previously administered PBS (n=8) (squares); uninfected BALB/c DEREG mice previously administered DTx (n=7) (triangles); uninfected BALB/c DEREG mice previously administered PBS (n=4) (diamonds); and BALB/c WT mice administered DTx prior to infection with *B. burgdorferi* (n=3) (cones). Error bars represent SEM.

Effect of Treg cell depletion on tibiotarsal joint swelling in B. burgdorferi-*infected mice.*

Average tibiotarsal joint measurements were obtained to assess edematous changes in

response to infection with *B. burgdorferi*. In one study, mice were infected with 1X10^2

spirochetes on the day immediately following the two consecutive days of DTx

administration. A minimal degree of swelling was observed in BALB/c DEREG mice

administered PBS prior to infection with 1X10^2 organisms (Figure 4). By contrast,

tibiotarsal joint swelling in BALB/c DEREG mice administered DTx prior to infection

increased consistently during the duration of the experiment. The tibiotarsal joint

31

swelling in BALB/c DEREG mice administered DTx prior to infection with 1×10^2 organisms was generally greater than that of BALB/c DEREG administered PBS prior to infection, approaching statistical significance ($P = 0.057$) at days 16 and 20 following infection. In addition, the degree of tibiotarsal joint swelling in BALB/c DEREG mice administered DTx prior to infection was also consistently greater than that of BALB/c WT mice administered DTx prior to infection, with statistically significant differences observed at day eight following infection and continuing for the remainder of the experiment ($P \leq 0.05$). No tibiotarsal joint swelling was observed in uninfected BALB/c DEREG mice administered DTx.
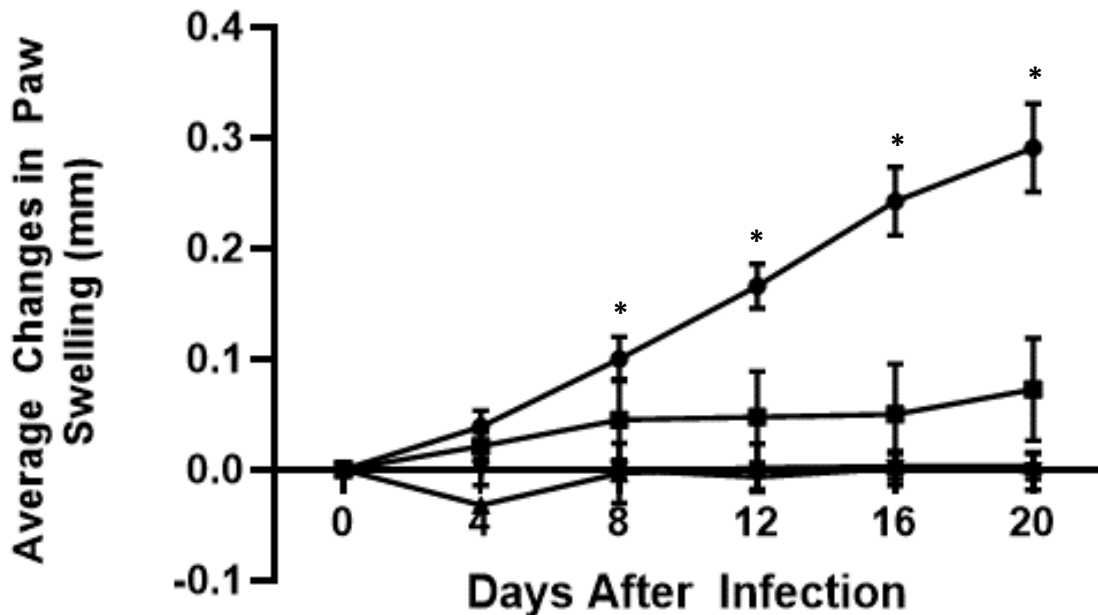
Figure 4. Average swelling changes in tibiotarsal joints of mice infected with 1×10^2 organisms. Groups consisted of *B. burgdorferi*-infected BALB/c DEREG mice previously administered DTx (n=4) (circles); *B. burgdorferi*-infected BALB/c DEREG mice previously administered PBS (n=4) (squares); uninfected BALB/c DEREG mice previously administered DTx (n=3) (triangles); *and B. burgdorferi*-infected BALB/c WT mice previously administered DTx (n=4) (cones). Error bars represent SEM. * $P \leq 0.05$ and denote a comparison between *B. burgdorferi*-infected BALB/c DEREG and WT mice administered DTx. Note: four lines are present on the graph, but no changes in paw measurements were observed in one group, so the fourth line overlaps both the third line and the x-axis .

In another study, the effects of Treg cell depletion were assessed in mice infected with 1×10^3 organisms. Increased swelling has been observed at increasing infectious doses (Figure 1; Ma *et al*. 1998), so it was predicted that similar results would be observed at an increased infectious dose. In BALB/c DEREG mice administered PBS prior to infection with *B. burgdorferi*, changes in tibiotarsal joint swelling were observed on day 8 following infection. This swelling increased steadily until day 28 after infection, at which point the swelling began to slightly decrease until day 35 following infection (Figure 5). Tibiotarsal joint swelling was also evident in BALB/c DEREG mice administered DTx prior to infection. Tibiotarsal joint swelling in these mice also became apparent on day 8 following infection and increased steadily until 32 days after infection before plateauing. However, no significant differences in tibiotarsal joint swelling were observed between these groups of mice. Tibiotarsal joint swelling was also observed in BALB/c WT mice administered DTx prior to infection. Tibiotarsal joint swelling in these mice became evident on day 8 following infection and continued increasing until day 28 following infection. Following this, a noticeable decrease in swelling was observed. Tibiotarsal joint swelling differences between *B. burgdorferi*-infected BALB/c DEREG and WT mice previously administered DTx approached statistical significance on day 32 following infection ($P = 0.06$) and reached statistical significance on day 35 after infection ($P \leq 0.05$). No tibiotarsal joint swelling was observed in either uninfected BALB/c DEREG mice previously administered DTx or in uninfected BALB/c DEREG mice previously administered PBS.
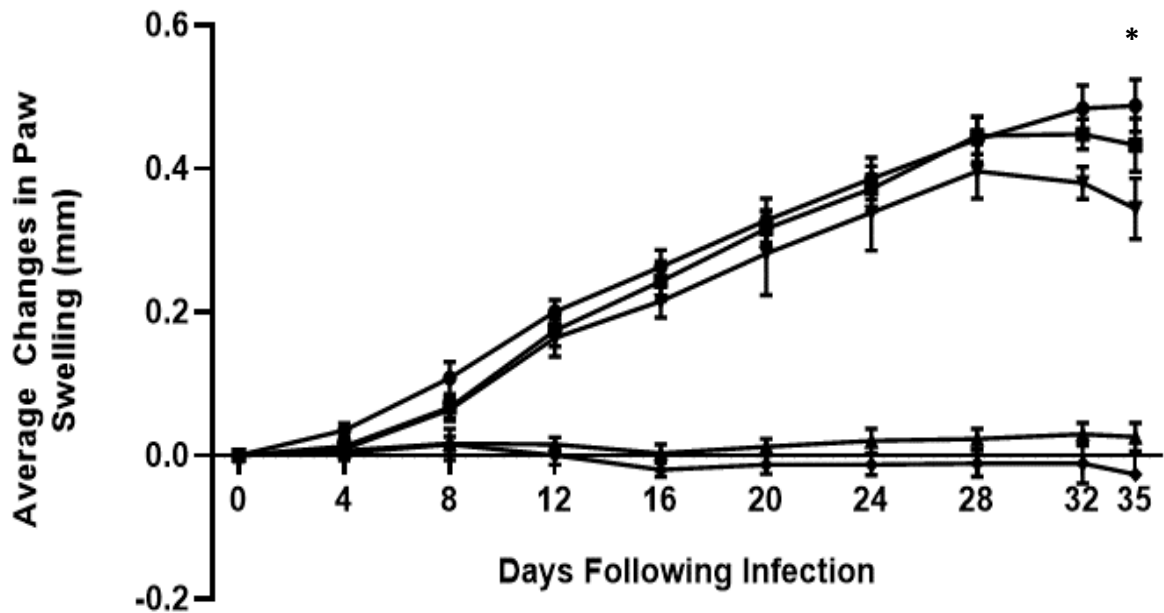
Figure 5. Average swelling changes in tibiotarsal joints of mice infected with 1X10³ organisms. Groups consisted of *B. burgdorferi*-infected BALB/c DEREG mice previously depleted of Treg cells (n=7) (circles); *B. burgdorferi*-infected BALB/c DEREG mice previously administered PBS (n=8) (squares); uninfected BALB/c DEREG mice administered DTx (n=7) (triangles); uninfected BALB/c DEREG mice administered PBS (n=3) (diamonds); and *B. burgdorferi*-infected BALB/c WT mice previously administered DTx (n=4) (cones). Error bars represent SEM. * P ≤ 0.05 and denote a comparison between *B. burgdorferi*-infected BALB/c DEREG and WT mice previously administered DTx.

Effect of Treg cell depletion on histopathology of tibiotarsal joints. The effect of Treg cell

depletion on the development of arthritis was assessed in mice infected with 1X10²

organisms. Histopathological analysis of the tibiotarsal joints revealed the presence of

minimal arthritic lesions in *B. burgdorferi*-infected BALB/c DEREG mice previously

administered PBS (Table 2). Additionally, minimal arthritis was found in *B. burgdorferi*-

infected BALB/c DEREG previously administered DTx. No statistically significant

differences were observed between these two groups. Likewise, histopathological

analysis revealed the presence of minimal arthritic lesions in *B. burgdorferi*-infected

BALB/c WT mice previously administered DTx. No statistically significant differences

were observed between infected BALB/c DEREG and WT mice previously administered

DTx. No arthritic lesions were observed in uninfected BALB/c DEREG mice

administered DTx.

Table 2: Average pathology scores of tibiotarsal joints in mice infected with $1X10^2$ spirochetes. Groups consisted of *B. burgdorferi*-infected BALB/c DEREG mice previously administered PBS (PBS + Bb) (n=4); *B. burgdorferi*-infected BALB/c DEREG mice previously depleted of Treg cells (DTx + Bb) (n=4); *B. burgdorferi*-infected BALB/c WT mice previously administered DTx (DTx + Bb) (n=4); and uninfected (PBS + normal mouse serum, NMS) BALB/c DEREG mice administered DTx (DTx) (n=3). Data presented as average scores ± SEM.

Genotype	DTx	Infection	Avg. Pathology Score
DEREG	PBS	Bb	0.33 ± 0.33
DEREG	DTx	Bb	0.50 ± 0.29
WT	DTx	Bb	0.25 ± 0.25
DEREG	DTx	PBS + NMS	0 ± 0

The effect of Treg cell depletion on the development of arthritis was also assessed in

mice infected with $1X10^3$ organisms. Histopathological analysis of the tibiotarsal joints

in *B. burgdorferi*-infected BALB/c DEREG mice previously administered PBS revealed

the presence of minimal arthritic lesions (Table 3). By contrast, two to three small foci

of inflammation were observed in multiple *B. burgdorferi*-infected BALB/c DEREG mice

previously administered DTx. However, no statistically significant pathological

differences were observed between these mice. Additionally, no arthritic lesions were

detected in *B. burgdorferi*-infected BALB/c WT mice previously administered DTx, and

no statistically significant differences were observed between these WT mice and

infected BALB/c DEREG mice previously administered DTx. No arthritis was detected

in either uninfected BALB/c DEREG mice previously administered DTx or in uninfected

BALB/c DEREG mice previously administered PBS.

Table 3: Average pathology scores of tibiotarsal joints in mice infected with 1X10³ spirochetes. Groups consisted of *B. burgdorferi*-infected BALB/c DEREG mice previously administered PBS (Bb + PBS) (n=8); *B. burgdorferi*-infected BALB/c DEREG mice previously depleted of Treg cells (DTx + Bb) (n=7); *B. burgdorferi*-infected BALB/c WT mice previously administered DTx (DTx + Bb) (n=4); uninfected BALB/c DEREG mice administered DTx (DTx + PBS + NMS) (n=7); and uninfected BALB/c DEREG mice administered PBS (PBS + PBS/NMS) (n=3). Data presented as average scores ± SEM. Note: one extreme outlying point was excluded from uninfected DEREG mice previously administered DTx (DTx + PBS/NMS). Removal of this point did not affect the statistical analysis.

Genotype	DTx	Infection	Avg. Pathology Score
DEREG	PBS	Bb	0.13 ± 0.13
DEREG	DTx	Bb	0.71 ± 0.36
WT	DTx	Bb	0 ± 0
DEREG	DTx	PBS + NMS	0.17 ± 0.17
DEREG	PBS	PBS + NMS	0 ± 0

III. Specific Aim 2: Determine the effect of Treg cells on the control of the immune response following infection with *B. burgdorferi*

Effect of Treg cell depletion on bacterial load in tibiotarsal joint tissue of infected mice.

qPCR analysis was used to quantify the levels of *B. burgdorferi* in the tibiotarsal joints

obtained from infected mice previously administered DTx to assess the impact of Treg

cells on the ability of the immune system to control dissemination of organisms. In one

study, in mice infected with 1X10² organisms, the bacterial load was assessed at 20

days following infection. No spirochetes were detected in *B. burgdorferi*-infected

BALB/c DEREG mice previously administered PBS (Figure 6). By contrast, the levels of

B. burgdorferi in the tibiotarsal joints of infected BALB/c DEREG mice previously

administered DTx was greater than those found in *B. burgdorferi*-infected BALB/c

DEREG mice administered PBS, but were low, overall; however, this increase was not

statistically significant. Lower levels of *B. burgdorferi* were detected in BALB/c WT mice

administered DTx prior to infection than in BALB/c DEREG mice administered DTx prior

to infection; however, this difference was also not statistically significant. No

spirochetes were detected in uninfected BALB/c DEREG mice administered DTx.
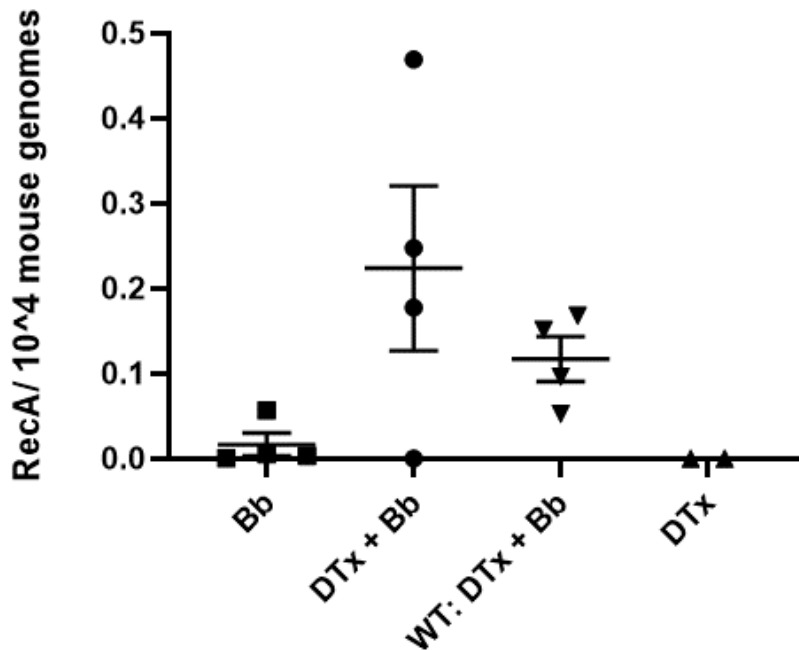
Figure 6. Borrelial load in tibiotarsal joint tissue of mice infected with 1X10^2 organisms. Groups consisted of BALB/c DEREG mice administered PBS prior to infection with *B. burgdorferi* (Bb) (n=4); BALB/c DEREG mice administered DTx prior to infection with *B. burgdorferi* (DTx + Bb) (n=4); *B. burgdorferi*-infected BALB/c WT mice previously administered DTx (WT) (n=4); and uninfected BALB/c DEREG mice previously administered DTx (DTx) (n=3). Data presented as average borrelial genomes (RecA) per 10^4 mouse genomes. Error bars represent SEM.

In another study, bacterial load was assessed in the tibiotarsal joints of mice infected with $1X10^3$ organisms at 35 days following infection. Low levels of spirochetes were detected in *B. burgdorferi*-infected BALB/c DEREG mice previously administered PBS (Figure 7). The levels of *B. burgdorferi* in infected BALB/c DEREG mice previously administered DTx were similar to those observed in infected BALB/c DEREG mice previously administered PBS, with no statistically significant differences between the two groups. Similarly, the levels of spirochetes detected in infected BALB/c WT mice previously administered DTx were comparable to those observed in infected BALB/c DEREG mice previously administered DTx, also with no statistically significant differences occurring between these two groups. No spirochetes were detected in either uninfected BALB/c DEREG mice previously administered DTx or in uninfected BALB/c DEREG mice previously administered PBS.
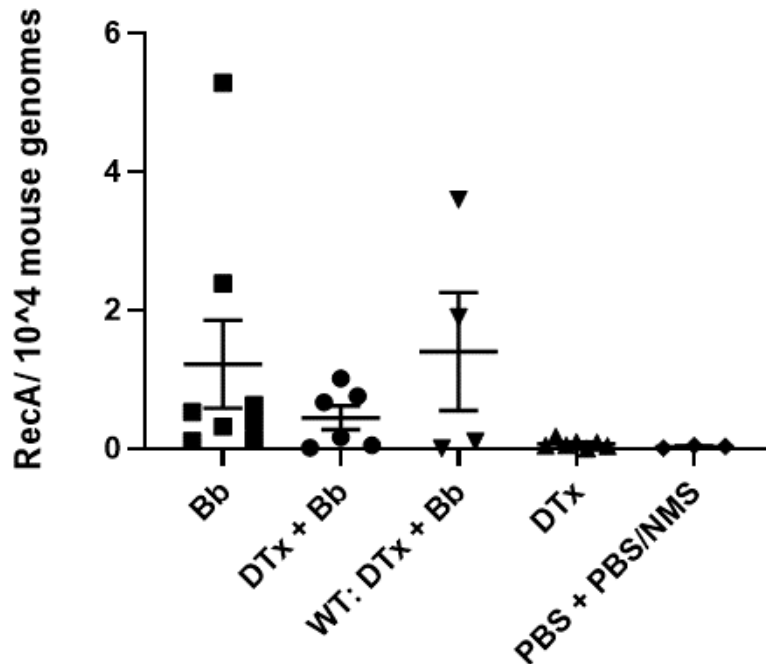
Figure 7. Borrelial load in tibiotarsal joint tissue of mice infected with $1X10^3$ organisms. Experimental groups consisted of BALB/c DEREG mice administered PBS prior to infection with *B. burgdorferi* (Bb) (n=8); BALB/c DEREG mice administered DTx prior to infection with *B. burgdorferi* (DTx + Bb) (n=6); *B. burgdorferi*-infected BALB/c WT mice previously administered DTx (WT) (n=4); uninfected BALB/c DEREG mice previously administered DTx (DTx) (n=7); and uninfected BALB/c DEREG mice previously administered PBS (PBS + NMS) (n=3). Data is presented as average borrelial genomes (RecA) per 10^4 mouse genomes. Error bars represent SEM.
Note: one extreme outlying data point (406 RecA/10^4 mouse genomes) was removed from the DTx + Bb group. Removal of this point did not affect the statistical analysis.

Effect of Treg cell depletion on bacterial load in heart tissue of infected mice

administered DTx. qPCR analysis was also used to quantify the levels of *B. burgdorferi*

in the heart tissue obtained from infected mice previously administered DTx. In mice

infected with $1X10^2$ organisms, the bacterial load was assessed at 20 days following

infection. Few spirochetes were detected in *B. burgdorferi*-infected BALB/c DEREG

mice administered PBS (Figure 8). The levels of *B. burgdorferi* in the heart tissue of

infected BALB/c DEREG mice previously administered DTx was similar to that found in

B. burgdorferi-infected BALB/c DEREG mice previously administered PBS, with no

statistically significant differences observed between these two groups. By contrast, no

spirochetes were detected in infected BALB/c WT mice previously administered DTx;

however, no statistically significant difference was observed between these mice and

infected BALB/c DEREG mice previously administered DTx. No spirochetes were

detected in uninfected BALB/c DEREG mice administered DTx.
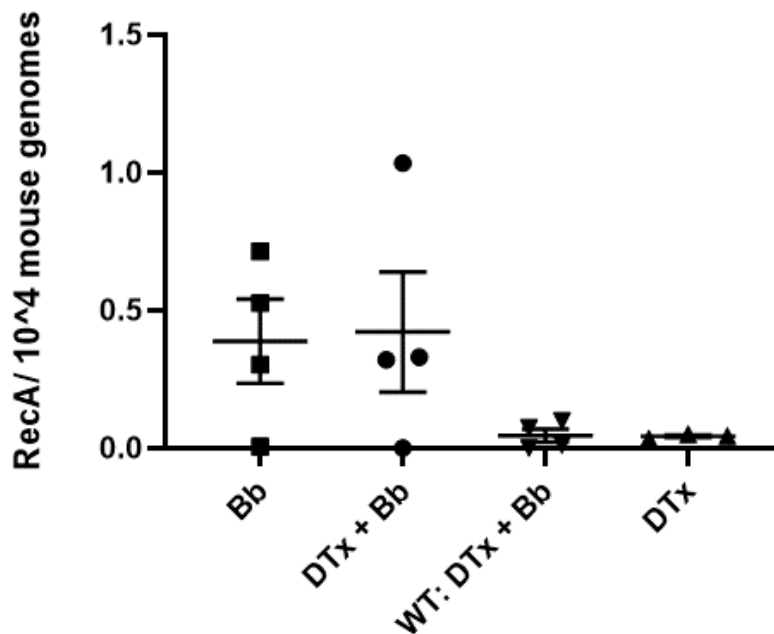
Figure 8. Borrelial load in heart tissue of mice infected with $1X10^2$ organisms. Groups consisted of BALB/c DEREG mice administered PBS prior to infection with *B. burgdorferi* (Bb) (n=4); BALB/c DEREG mice administered DTx prior to infection with *B. burgdorferi* (DTx + Bb) (n=4); *B. burgdorferi*-infected BALB/c WT mice previously administered DTx (WT) (n=4); and uninfected BALB/c DEREG mice previously administered DTx (DTx) (n=3). Data presented as average borrelial genomes (RecA) per 10^4 mouse genomes. Error bars represent SEM.

In another study, bacterial load was assessed in the heart tissue of mice infected with

$1X10^3$ organisms at 35 days following infection. Few spirochetes were detected in *B.*

burgdorferi-infected BALB/c DEREG mice previously administered PBS (Figure 9). By

contrast, the levels of *B. burgdorferi* in infected BALB/c DEREG mice previously administered DTx were significantly greater than those observed in infected BALB/c DEREG mice previously administered PBS (P ≤ 0.01); however, the borrelial load in these mice was still relatively small. In addition, levels of spirochetes detected in infected BALB/c WT mice previously administered DTx were significantly lower than those of infected BALB/c DEREG mice previously administered DTx (P ≤ 0.05). No spirochetes were detected in either uninfected BALB/c DEREG mice previously administered DTx or in uninfected BALB/c DEREG mice previously administered PBS.
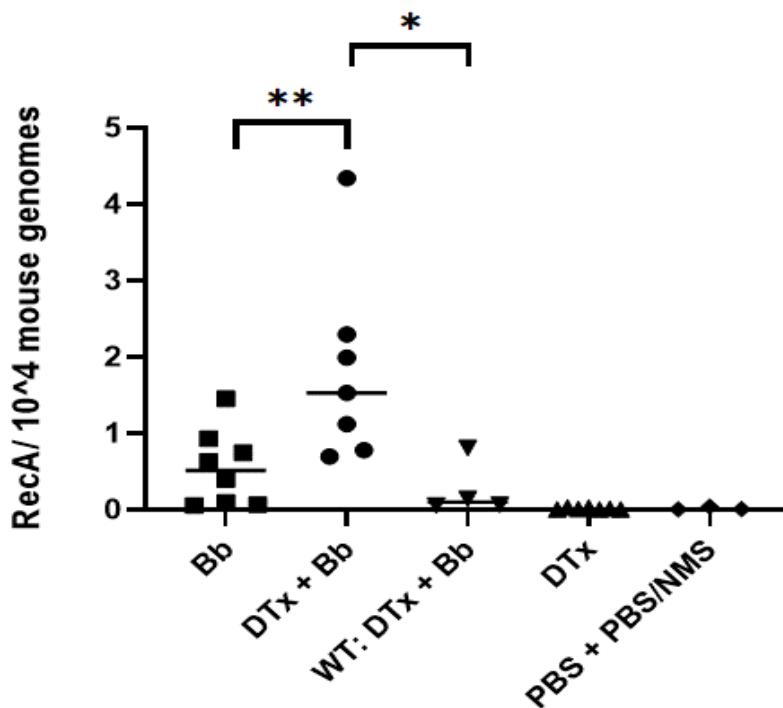
Figure 9. Borrelial load in heart tissue of mice infected with 1X10⁵ organisms. Experimental groups consisted of BALB/c DEREG mice administered PBS prior to infection with *B. burgdorferi* (Bb) (n=8); BALB/c DEREG mice previously administered DTx prior to infection with *B. burgdorferi* (DTx + Bb) (n=6); *B. burgdorferi*-infected BALB/c WT mice previously administered DTx (WT) (n=4); uninfected BALB/c DEREG mice previously administered DTx (DTx) (n=7); and uninfected BALB/c DEREG mice previously administered PBS (PBS + PBS/NMS) (n=3). Data is presented as average borrelial genomes (RecA) per 10^4 mouse genomes. Error bars represent SEM. * P-values ≤ 0.05. ** P-value ≤ 0.01.

Effect of Treg cell depletion on cytokine levels in serum. A multiplex cytokine assay was used to determine the concentration of twelve cytokines in the serum of *B. burgdorferi*-infected DEREG mice previously administered diphtheria toxin or not administered diphtheria toxin. The majority of cytokines analyzed were not detected in the serum samples (data not shown); however, IL-4, IL-5, and IL-10 were detected at concentrations that fell within the range of the respective standard curves for each cytokine. IL-4 was the most abundant cytokine detected in the serum of all groups of mice. The concentration of IL-4 in *B. burgdorferi*-infected BALB/c DEREG mice previously administered PBS tended to be higher than the concentration detected in *B. burgdorferi*-infected BALB/c DEREG mice previously administered DTx; however, this difference was not statistically significant (Figure 10A). Additionally, the concentration of IL-4 was also similar in infected BALB/c DEREG and WT mice previously administered DTx, with no statistically significant difference between these two groups. The concentrations of IL-4 in uninfected BALB/c DEREG mice previously administered DTx or not previously administered DTx were comparable to those observed in infected BALB/c DEREG mice previously administered PBS. By contrast, in naïve mice, which were mice that had not been subjected to any treatments during the experiment, the highest concentration of IL-4 was detected. None of these differences were statistically significant.

IL-5 also was detected in the serum of all groups of mice. The concentration of IL-5 in *B. burgdorferi*-infected BALB/c DEREG mice previously administered PBS was lower than the concentration detected in *B. burgdorferi*-infected BALB/c DEREG mice

previously administered DTx; however, this difference was not statistically significant (Figure 10B). Additionally, the concentration of IL-5 in infected BALB/c DEREG mice previously administered DTx was higher than that detected in infected BALB/c WT mice previously administered DTx; however, no statistically significant difference was observed between these two groups. By contrast, in uninfected BALB/c DEREG mice previously administered DTx, the concentration of IL-5 tended to be greater than all other groups. In uninfected BALB/c mice previously administered PBS, the concentration of IL-5 observed in the serum tended to be lower than all other groups. A comparable concentration of IL-5 was detected in naïve mice and both infected BALB/c DEREG mice previously administered PBS and infected BALB/c WT mice previously administered DTx.

IL-10 was also detected in the serum of mice. The concentration of IL-10 in *B. burgdorferi*-infected BALB/c DEREG mice previously administered PBS was slightly lower than that detected in *B. burgdorferi*-infected BALB/c DEREG mice previously administered DTx; however, this difference was not statistically significant (Figure 10C). By contrast, the concentration of IL-10 in infected BALB/c DEREG mice administered DTx prior to infection was significantly higher than that detected in infected BALB/c WT mice previously administered DTx (P ≤ 0.05). No IL-10 was observed in the serum of uninfected BALB/c DEREG mice previously administered DTx. Slightly lower concentrations of IL-10 were observed in uninfected BALB/c DEREG mice previously administered PBS than in BALB/c DEREG mice administered PBS prior to infection. Minimal IL-10 was observed in naïve mice.
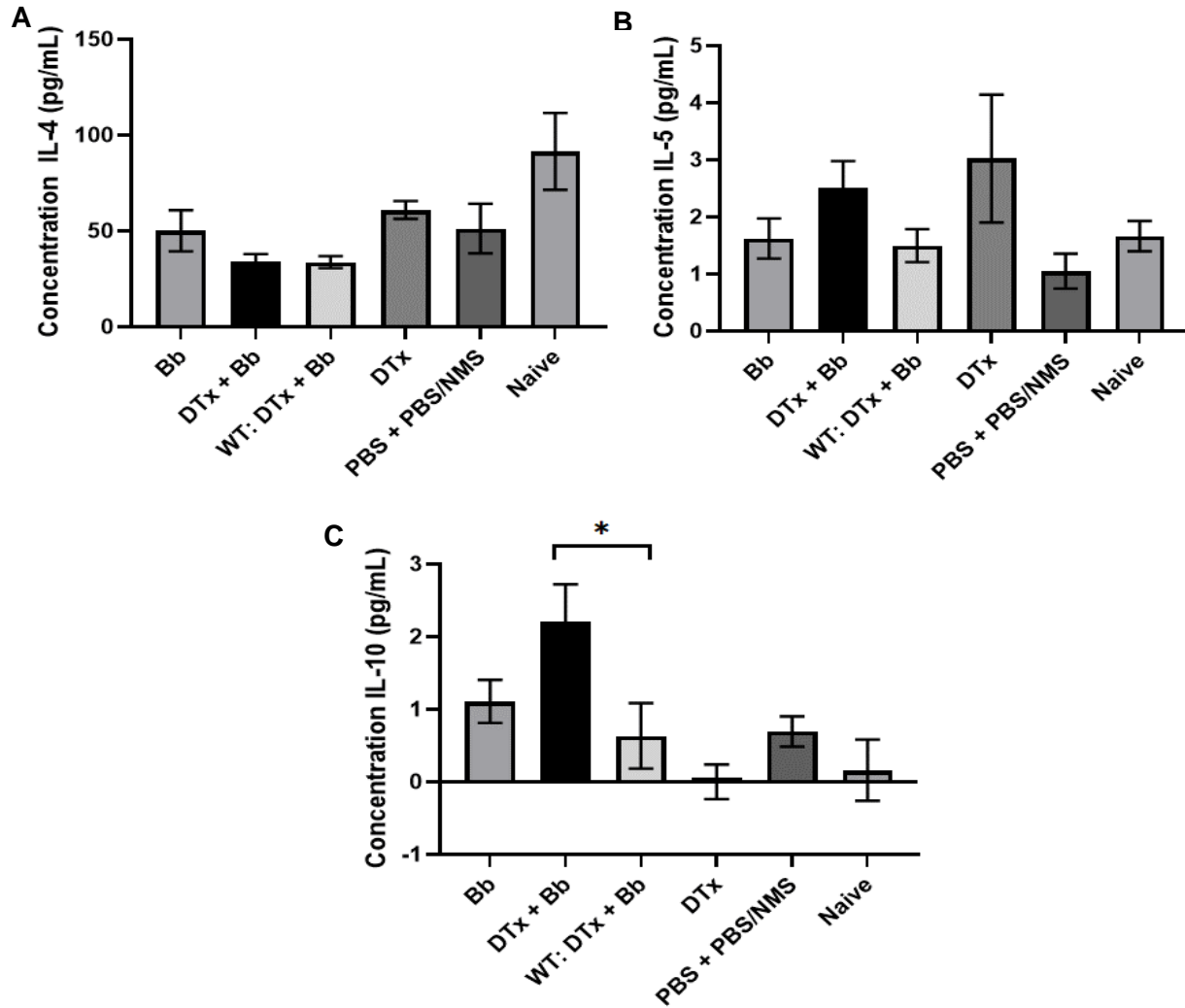
Figure 10. IL-4 (A), IL-5 (B), and IL-10 (C) concentrations detected in serum of either uninfected or infected mice not administered DTx or administered DTx. Groups consisted of BALB/c DEREG mice administered PBS prior to infection with *B. burgdorferi* (Bb) (n=8); BALB/c DEREG mice depleted of Treg cells prior to infection with *B. burgdorferi* (DTx + Bb) (n=7); *B. burgdorferi*-infected BALB/c WT mice administered DTx (WT: DTx + Bb) (n=4); uninfected BALB/c DEREG mice administered DTx (DTx) (n=7); uninfected BALB/c DEREG mice administered PBS (PBS + PBS/NMS) (n=3); and untreated naïve mice (naïve) (n=3). Data presented as average concentration (pg/mL) of cytokine per group. Error bars represent SEM. * P-values < 0.05.

CHAPTER 4: DISCUSSION

Little evidence exists of the role of Treg cells within the context of the development and progression of Lyme disease. Additionally, little evidence exists of the role of Treg cells in the control of the immune response to infection with *B. burgdorferi*. The objective of this thesis was to determine the role of Treg cells in the development and progression of Lyme disease in a disease-susceptible mouse model. We hypothesized that Treg cells control the development and progression of Lyme disease following *B. burgdorferi* infection. To test this hypothesis, the first specific aim was to determine the effect of Treg cells on the development of arthritis following infection with *B. burgdorferi*, with the working hypothesis that depletion of Treg cells will exacerbate tibiotarsal joint swelling and arthritis. The second specific aim pursued was to determine the effect of Treg cells on the control of the immune response following infection with *B. burgdorferi*, with the working hypothesis that depletion of Treg cells will result in an increased ability to control bacterial dissemination and increased levels of pro-inflammatory cytokines following *B. burgdorferi* infection. We demonstrated that depletion of Treg cells immediately prior to infection of BALB/c mice with *B. burgdorferi* led to significantly increased edema in the tibiotarsal joints of mice infected with a low dose of organisms (Figures 4 and 5), with indications of increased arthritis among some mice (Table 3). We also demonstrated that Treg cell depletion affected the ability of the immune system to prevent bacterial dissemination as higher levels of *B. burgdorferi* were observed in tissues of mice that had been administered diphtheria toxin prior to infection (Figures 6 and 9) .

All studies, with the exception of the preliminary experiment, were conducted using the "depletion of regulatory T cell", or DEREG, mouse model on the BALB/c background. The DEREG mouse strain has been engineered to express a fusion protein comprised of a diphtheria toxin receptor and an enhanced green fluorescent protein which is under the control of the *foxp3* promoter (Lahl *et al.* 2007). As Foxp3 is regarded as the definitive marker for identification of Treg cells (Fontenot *et al.* 2003), this mouse model allows for the selective depletion of Treg cells via administration of small amounts of diphtheria toxin. In fact, the vast majority of Foxp3$^+$ Treg cells are depleted with two consecutive days of injection with 1 µg of DTx (Lahl and Sparwasser 2011), thus enabling researchers to study the role of Treg cells in a variety of diseases. In support of this, we assessed the Treg cell depletion efficiency the day after two consecutive days of administration of two lots of DTx. The two lots of DTx reduced the amounts of Foxp3$^+$ cells by approximately 75% and 80%, respectively (Table 1). BALB/c WT mice, in which diphtheria toxin would have no effect on Treg cells, were used as additional controls. It was expected that these BALB/c WT mice would exhibit disease in a manner similar to BALB/c DEREG mice infected with *B. burgdorferi* and administered PBS alone. This hypothesis was supported by the observation of similar trends in tibiotarsal joint swelling, arthritis development, borrelial loads, and serum cytokine profiles, with no significant differences observed between these two groups.

Weight changes were recorded during all studies involving the use of diphtheria toxin. A common side effect of injection with small amounts of diphtheria toxin is transient weight loss (Mayer *et al.* 2014). BALB/c WT mice allowed for the monitoring of potential

toxicity induced by injection of diphtheria toxin. A delay in weight gain and, in some instances, transient weight loss were observed in all mice administered diphtheria toxin, whereas mice not administered diphtheria toxin exhibited consistent weight gain for the duration of the experiments (Figures 2 and 3). Any weight loss occurred immediately following administration of the toxin, and then the mice began to gain weight within a week following injection. This trend was similar across all mice that had been administered diphtheria toxin regardless of genotype. This finding was corroborated by previous studies using DEREG mice in our lab, in which similar trends were observed in C57BL/6 DEREG mice following diphtheria toxin administration (Nardelli *et al.* unpublished data). This observation suggested that any effects observed in the disease severity of *B. burgdorferi*-infected DEREG mice administered diphtheria toxin would be due to the effects of Treg cell depletion on infection and not due to any adverse health effects associated with diphtheria toxin administration. This was also corroborated by the lack of tibiotarsal joint swelling observed in uninfected BALB/c DEREG mice administered DTx (Figures 4 and 5).

In one study, BALB/c DEREG mice were administered DTx prior to infection with 1×10^2 spirochetes, with a group of BALB/c DEREG mice administered PBS prior to infection serving to demonstrate the normal progression of infection in the presence of Treg cells. Based on timing of the appearance of tibiotarsal joint swelling in the preliminary experiment (Figure 1), 20 days following infection was chosen as the experimental end point. Ma *et al.* (1998) showed that WT BALB/c mice infected with 2×10^2 spirochetes did not previously exhibit ankle joint swelling; therefore, it was predicted that infection

with this dose may allow for visualization of any effects of Treg cell depletion on disease. Here, in BALB/c DEREG mice administered PBS prior to infection with $1X10^2$ spirochetes, no edematous changes in the tibiotarsal joint were also observed.

Additionally, no tibiotarsal joint swelling was observed in infected WT mice previously administered DTx. By contrast, joint swelling was apparent in *B. burgdorferi*-infected BALB/c DEREG mice previously administered DTx (Figure 4). The difference in joint swelling between infected DEREG and WT mice previously administered DTx was statistically significant from Day 8 through Day 20 following infection (Figure 4, P ≤ 0.05). Additionally, the differences in paw swelling between BALB/c DEREG mice depleted of Treg cells prior to infection and infected BALB/c DEREG mice not previously depleted of Treg cells approached statistical significance by days 16 and 20 following infection (P = 0.057). It is possible that statistical significance was not achieved between these two groups because one mouse that had been administered PBS prior to infection exhibited a minimal degree of tibiotarsal joint swelling. Our findings that depletion of Treg cells increased tibiotarsal joint swelling in *B. burgdorferi*-infected BALB/c mice are supported by previous studies in our lab. Our lab demonstrated that depletion of Treg cells in infected, Lyme arthritis-resistant C57BL/6 mice also led to significantly greater paw swelling than *B. burgdorferi*-infected C57BL/6 mice administered PBS alone (Nardelli *et al*. unpublished data). These findings also provide support for use of the DEREG mouse model, since the differences in tibiotarsal joint swelling observed between infected BALB/c WT mice and the BALB/c DEREG mice administered DTx were due to the specific depletion of the Treg cells that occurred in the DEREG mice and not due to differences in weight loss.

Hind paw swelling is not necessarily indicative of arthritis but is instead more indicative

of edema associated with the inflammatory response (Ma *et al.* 1998). However,

tibiotarsal joint swelling has occasionally been correlated with the development of

arthritis, with increased paw swelling corresponding to arthritis severity (Glickstein *et al.*

2001). Based on the paw swelling data obtained from mice infected with $1X10^2$

organisms, it was expected that the depletion of Treg cells would lead to the

development and increased severity of Lyme arthritis. However, pathological

assessment of the tibiotarsal joints in mice infected with $1X10^2$ spirochetes did not

reveal the presence of arthritic lesions in any of the infected mice (Table 2). This finding

was unexpected given the substantially increased paw swelling observed in the mice

depleted of Treg cells. Although unexpected, these findings may be supported by Ma *et*

al. (1998), in which arthritis development was not observed in BALB/c mice infected with

$2X10^2$ organisms at 28 days following infection. It is possible that, even though paw

swelling was observed in this study, $1X10^2$ organisms may have been too low of a dose

of organisms to elicit a pathological response, even in the absence of Treg cells.

Additionally, it is possible that as disease progressed and inflammation continued in the

tibiotarsal joint tissue, that arthritis would begin to develop with a longer experimental

duration. Twenty days may not have been long enough for arthritis to develop.

We and others have demonstrated that tibiotarsal joint swelling increases with

increasing infectious doses of *B. burgdorferi* in BALB/c mice (Figure 1; Ma *et al.* 1998).

In another study, $1X10^3$ *B. burgdorferi* organisms were used and 35 days was chosen

as the experimental end point to assess the effects of Treg cell depletion. Infection of

BALB/c mice with $1\text{X}10^3$ organisms has been shown to induce a mild degree of tibiotarsal joint swelling (Figure 1; Ma *et al*. 1998). We predicted that mice infected with $1\text{X}10^3$ organisms would also exhibit paw swelling, with depletion of Treg cells leading to increased edematous changes and the development of arthritis. However, at the infectious dose of $1\text{X}10^3$ *B. burgdorferi*, there were no statistically significant differences observed in tibiotarsal joint swelling between infected BALB/c DEREG mice previously administered PBS and infected BALB/c DEREG mice administered DTx, although the degree of swelling eventually was slightly greater in the DEREG mice depleted of Treg cells. We observed that the joint swelling in infected mice previously depleted of Treg cells continued to increase throughout the duration of the experiment, whereas the joint swelling of infected mice not depleted of Treg cells began to subside by the end of the experiment. In addition, the swelling differences observed between infected BALB/c DEREG mice previously administered DTx and infected BALB/c WT mice previously administered DTx was greater and approached statistical significance by Day 32 (P = 0.06), reaching statistical significance by day 35 (P ≤ 0.05) following infection (Figure 5). Therefore, Treg cells also appeared to control the development of swelling in BALB/c mice infected with $1\text{X}10^3$ *B. burgdorferi*, although not to the degree that was observed at the lower infectious dose.

Based on the degree of swelling observed in mice infected with $1\text{X}10^3$ organisms, we predicted that these mice would develop mild arthritis, with depletion of Treg cells resulting in increased arthritis severity. Pathological analysis revealed the presence of two to three small foci of inflammation in the tibiotarsal joints of some BALB/c DEREG

mice depleted of Treg cells prior to infection with *B. burgdorferi*, with little pathology observed in other mice belonging to this group. By contrast, no arthritic lesions were detected in other groups of mice (Table 3). It has been demonstrated that the degree of tibiotarsal joint swelling in BALB/c mice infected with $1X10^3$ *B. burgdorferi* is mild (Figure 1). In addition, arthritis that develops in BALB/c mice infected with $2X10^3$ organisms was also demonstrated to be mild (Ma *et al*. 1998). In general, BALB/c mice have been regarded as resistant to the development of Lyme arthritis as infection with $1X10^6$ or $1X10^7$ organisms led to the development of only mild to moderate arthritis (Barthold *et al*. 1990). Subsequent studies have, however, demonstrated that arthritis development can be seen in BALB/c mice infected with lower doses of *B. burgdorferi*, including $2X10^4$ and $2X10^5$ organisms (Ma *et al*. 1998). Despite the increase in severity of arthritis observed by Ma *et al*, and despite the swelling observed with this infectious dose, these findings suggest that $1X10^3$ organisms may also not have been sufficient to fully observe effects of Treg cell depletion on development and severity of arthritis. However, we observed the development of moderate arthritis in approximately 30% of BALB/c DEREG mice depleted of Treg cells prior to infection with $1X10^3$ *B. burgdorferi*. This provides an indication that Treg cells may, indeed, be involved in inhibiting the development of actual pathology in these mice.

Collectively, our findings provide partial support for a role for Treg cells in the development and progression of Lyme disease. Although arthritis severity was not significantly worsened by ablation of Treg cells immediately prior to infection, the significantly increased joint swelling observed in BALB/c DEREG mice depleted of Treg

cells prior to infection with *B. burgdorferi* does provide support for the hypothesis. In our lab, depletion of Treg cells in C57BL/6 mice, a mouse genotype normally resistant to the development of arthritis, led to significantly increased paw swelling and differences in arthritis development approaching statistical significance (Nardelli *et al*. unpublished data). In initial experiments using BALB/ c mice, a more disease-susceptible mouse strain and low infectious doses, we provide evidence that Treg cells likely influence the development of joint swelling due to *B. burgdorferi* infection. We also began to observe the development of pathology among individual Treg cell-depleted, infected mice as we increased the infectious dose. The difference in results could potentially be attributed to the different mouse strains used. Previous studies in our lab were conducted using C57BL/6 mice, whereas these studies were conducted using BALB/c mice. Although both mouse models have been regarded as arthritis resistant, studies have demonstrated that these mouse models respond differently to infection with *B. burgdorferi*. It has been reported that the arthritis resistance in BALB/c mice can be overcome by high doses of inoculum, thereby leading to a disease phenotype more comparable to that seen in the highly susceptible C3H mouse (Ma *et al*. 1998). By contrast, disease severity was consistently mild in C57BL/6 mice, even when higher doses of inoculum had been used (Barthold *et al*. 1990; Ma *et al*. 1998), providing support for C57BL/6 mice as being a more Lyme disease resistant model than BALB/c mice. It has been postulated that these differences in response to infection are a result of inherent immunological differences present in these two mouse strains.

It is widely accepted that C57BL/6 mice are genetically biased towards a type 1 immune response, characterized by development of Th1 cells and secretion of their effector cytokines, such as IFN-γ. Conversely, BALB/c mice are predisposed towards development of a type 2 immune response, which is characterized by proliferation of Th2 cells and secretion of their effector cytokines, such as IL-4 (Watanabe *et al*. 2004). The differences observed in the effect of Treg cell depletion on Lyme disease in these two mouse strains could be explained by their respective genetic biases towards one type of immune response. Treg cells may impact Th1 and Th2 cells differently. For example, one study suggested that Th2 cells are less susceptible to suppression by CD4$^+$CD25$^+$ putative Treg cells than Th1 cells (Cosmi *et al*. 2004). This finding could explain why a more profound effect of Treg cell depletion was observed in C57BL/6 mice than in the BALB/c mice. The Th2 bias of BALB/c mice may not allow them to be as susceptible to suppression by Treg cells, so when the Treg cells were removed, no difference in disease severity was observed. Additionally, the differences observed in the effect of Treg cell depletion in these two mouse strains could be attributed to the infectious dose used. An infectious dose of 2×10^4 *B. burgdorferi* organisms was used in the C57BL/6 mice (Nardelli *et al*. unpublished data), which was considerably higher than the infectious doses of 1×10^2 and 1×10^3 organisms used in these studies.

The lack of functional Treg cells can lead to a dysregulated immune response, contributing to the pathogenesis of various autoimmune diseases (Sakaguchi *et al*. 2008); therefore, we also assessed the effect of Treg cell depletion on the immune response to infection with *B. burgdorferi*. The borrelial load in tibiotarsal joint tissue and

heart tissue was quantified as one measure of the effect of Treg cell depletion on the immune response to infection.   At the infectious dose of $1X10^2$ organisms, the levels of *B. burgdorferi* found in infected DEREG mice previously administered DTx were slightly greater in the tibiotarsal joint than either infected DEREG mice not previously administered DTx or infected WT mice previously administered diphtheria toxin (Figure 6). Additionally, in the ankle joints of all groups of mice infected with either $1X10^2$ or $1X10^3$ organisms, the borrelial load appeared to corroborate the tibiotarsal joint swelling results, with higher levels of spirochetes correlating with the increased joint swelling. In the heart tissue of mice infected with $1X10^2$ organisms, no differences in borrelial load were observed between infected DEREG mice administered DTx and either infected DEREG mice administered PBS or infected WT mice administered PBS (Figure 8). However, in the heart tissue of mice infected with $1X10^3$ organisms, the levels of *B. burgdorferi* found in DEREG mice administered DTx prior to infection were greater than the levels observed in the heart tissue of either infected DEREG mice previously administered PBS or infected WT mice previously administered DTx, with statistically significant differences between infected DEREG mice previously administered DTx and infected mice previously administered PBS (Figure 9; $P \leq 0.01$) and also between infected DEREG mice administered DTx and infected WT mice previously administered DTx (Figure 9; $P \leq 0.05$). The increased levels of *B. burgdorferi* detected in infected DEREG mice previously administered DTx suggest that the depletion of Treg cells may potentially affect the immune system's ability to clear *B. burgdorferi*, thereby allowing the organism to disseminate throughout the body.

Cells of the innate immune system, such as neutrophils and macrophages have been shown to be involved in phagocytosis and killing of *B. burgdorferi* and have been observed in areas of inflammation (Benach *et al*. 1984; Barthold *et al*. 1991). Additionally, B cells have been shown to be responsible for the resolution of Lyme arthritis and carditis (McKisic and Barthold 2000). Specifically, a robust B cell response has been shown to result in a more rapid resolution of disease (Blum *et al*. 2018). BALB/c mice are believed to generate a strong B cell response to infection with *B. burgdorferi* (Glickstein *et al*. 2001). It has also been suggested that borreliacidal antibody production is important for protection against *B. burgdorferi*, as presence of these antibodies correlates with elimination of spirochetes from tissues (Creson *et al*. 1996). The primary mechanism by which Treg cells control the immune response is secretion of anti-inflammatory cytokines. It has been suggested that secretion of TGF-β by Treg cells affects the proliferation of T and B cells, and also affects the activity of macrophages, dendritic cells, and natural killer cells (Yoshimura *et al*. 2010). It is possible that depletion of Treg cells would lead to decreased production of TGF-β, which would increase the proliferation of innate immune cells and the production of antibodies. Theoretically, this increase in cells should then lead to a more robust immune response to infection with *B. burgdorferi*, thereby preventing the dissemination of spirochetes. However, *B. burgdorferi* has been shown to induce the production of the anti-inflammatory cytokine IL-10 by innate host cells (Giambartolomei *et al*. 1998; Brown *et al*. 1999; Ganapamo *et al*. 2003). Instead of the possibly increased numbers of innate cells contributing to spirochete control, depletion of Treg cells could possibly lead to the secretion of more IL-10 by these cell types. Increased levels of IL-10 would then

act to suppress the initial inflammatory response, thus allowing *B. burgdorferi* to evade destruction and migrate to other tissues. This could explain the increased concentrations of *B. burgdorferi* observed in the tibiotarsal joint of mice infected with $1X10^2$ organisms and the heart tissue of mice infected with $1X10^3$ organisms that were depleted of Treg cells (Figures 6 and 9). Even though the infectious doses were low, the organisms were able to disseminate, also causing the increased joint swelling observed in these mice (Figures 4 and 5).

Studies in other models of infection have also demonstrated that Treg cell depletion affects the clinical outcomes of disease. A protective role for Treg cells has been demonstrated in some virally infected mice (Lund *et al*. 2008; Lanteri *et al*. 2009), some parasitic infections (Oldenhove *et al*. 2009; Haque *et al*. 2010), and some fungal infections (Pandiyan *et al*. 2011) as ablation of Treg cells in these infected mice have led to increased viral, parasitic, and fungal loads. Conversely, a detrimental role for Treg cells has been shown in other bacterial infections, such as *Listeria monocytogenes* and *Salmonella enterica*. In these infections, it was demonstrated that depletion of Treg cells resulted in decreased pathogen burden (Johanns *et al*. 2010; Rowe *et al*. 2011). Based on the assessment of borrelial load, Treg cells may serve a protective role in *B. burgdorferi* infection, as depletion of these cells led to increased borrelial load in both tibiotarsal joint and heart tissue. Further studies are needed to support this hypothesis.

The levels of *B. burgdorferi* found in both the joint and heart tissue were found to be relatively low; however, this may have been expected due to the low infectious dose

used for both studies. Additionally, the route of infection could potentially impact the course of disease. It has been suggested that BALB/c mice infected with *B. burgdorferi* directly into the footpad readily develop arthritis (Motameni *et al.* 2005). For our studies, mice were infected subcutaneously between the scapulae, so the bacteria had to disseminate to the joint tissue. It has been demonstrated that *B. burgdorferi* disseminate to areas more proximal to the site of inoculation, with fewer spirochetes travelling to distal sites (Motameni *et al.* 2005). However, many studies involved infecting mice intradermally at a site removed from the location of pathology as a way to model the bacterial dissemination that would occur in humans following a tick bite. BALB/c mice infected in this manner have also developed arthritis, but the infectious doses have been higher than those used in our studies (Barthold *et al.* 1990; Barthold *et al.* 1991; de Souza *et al.* 1993; Yang *et al.* 1994; Ma *et al.* 1998). The route of infection could impact disease outcomes in combination with the infectious dose. At these lower infectious doses, it is plausible that fewer spirochetes were able to disseminate from the site of infection, especially to the joint tissue; therefore, arthritis development generally was not observed. It is possible that more spirochetes disseminated to the heart tissue. Additionally, the levels of *B. burgdorferi* in both tissues appeared to be dependent upon the infectious dose used, as lower levels tended to be detected in mice infected with $1X10^2$ organisms than in mice infected with $1X10^3$ organisms (Figures 6-9). It has been suggested that severity of disease corresponds to the numbers of spirochetes within tissues, with persistence of higher numbers of spirochetes within the joint tissue corresponding to increased severity of Lyme arthritis (Yang *et al.* 1994). By contrast, in mice deficient for IL-10, fewer spirochetes were detected in joint tissue, but increased

arthritis severity was observed (Brown *et al.* 1999), suggesting that disease severity may not necessarily correlate with spirochete presence in tissues. Interestingly, *B. burgdorferi* stimulates the production of IL-10 early in response to infection (Giambartolomei *et al.* 1998; Brown *et al.* 1999; Ganapamo *et al.* 2003); therefore, it is possible that Treg cell depletion leads to increased numbers of innate immune cells, which increases the secretion of IL-10 in response to infection. This hypothesis is supported by the increased numbers of spirochetes detected in joint and heart tissue of *B. burgdorferi*-infected DEREG mice depleted of Treg cells (Figures 6-9).

To further determine the effect of Treg cell depletion on the immune response following *B. burgdorferi* infection, multiplex cytokine analysis was performed to determine the concentrations of various pro- and anti-inflammatory cytokines in mouse serum. As some pro-inflammatory cytokines have been implicated in the pathogenesis of Lyme arthritis, it was predicted that depletion of Treg cells would lead to increased concentrations of pro-inflammatory cytokines. Of particular interest were cytokines associated with Th1 and Th17 cells, namely IFN-γ and IL-17, respectively. IFN-γ (Yssel *et al.* 1991; Gross *et al.* 1998) and IL-17 (Codolo *et al.* 2013) were of particular interest due to their role in pathogenesis of Lyme arthritis in humans. Neither of these cytokines were detected in the serum of mice at concentrations that fell within the range of their respective standard curves (data not shown). It is possible that IFN-γ was not detected in BALB/c mice because it has been suggested that a Th1 response occurs earlier during the course of infection, with the Th1 immune response transitioning over to a Th2-dominated response approximately two weeks after infection (Kang *et al.* 1997).

Additionally, IFN-γ does not appear to be required for resistance to Lyme arthritis; however, ablation of IFN-γ does promote generation of a Th2 response over a Th1 response (Glickstein *et al.* 2001). It is also possible that the immunological bias of a Th2 immune response in BALB/c mice may prevent the development of a Th1-mediated response, as cytokines secreted by Th2 cells act as negative regulators of a Th1 response, thereby preventing differentiation of Th1 cells (Fishman and Perelson 1994). The low amount of pro-inflammatory cytokines detected in these mice could explain the overall lack of arthritis development. IL-4, IL-5, and IL-10 were, however, detected in the serum samples at concentrations within the ranges of their respective standard curves, providing further support for the inherent Th2 bias present in these mice.

IL-10 was one of the cytokines detected in mouse serum. IL-10 is an anti-inflammatory cytokine produced by a variety of cell types, with Treg cells being the most abundant source (Arce-Sillas *et al.* 2016). The role of IL-10 has been studied within the context of Lyme disease; however, many of these studies have been conducted in C57BL/6 mice, as IL-10 is believed to be an important contributing factor to resistance in this mouse model. A study conducted by Brown *et al.* (1999) demonstrated that IL-10 deficiency in C57BL/6 mice resulted in increased severity of arthritis, but decreased numbers of spirochetes in the joint tissue (Brown *et al.* 1999). A possible mechanism of regulation is that IL-10 leads to decreases in the inflammatory Th17 cell responses (Hansen *et al.* 2013), suggesting that IL-10 is responsible for the regulation of arthritis severity in the Lyme disease-resistant mouse model. Surprisingly, the highest level of IL-10 was observed in infected DEREG mice previously administered DTx. When compared to

infected WT mice previously administered DTx, the difference was statistically

significant. In the DEREG mouse model, Treg cells begin to rebound approximately

four days after depletion, with a complete rebound achieved by fourteen days after

depletion (Lahl and Sparwasser 2011). It is possible that the increased levels of IL-10

detected in the serum of infected mice previously depleted of Treg cells could be a

result of overcompensation of Treg cells as they rebounded in an attempt to regain

control of the immune response to infection. It is possible that IL-10, in conjunction with

IL-4, may serve to contribute to the regulation of disease severity in BALB/c mice.

However, Treg cells are not the only source of IL-10. It is possible that the IL-10

observed in serum did not originate from Treg cells, but instead may have originated

from the Th2 cells as part of a regulatory mechanism to prevent the differentiation of

Th1 cells (Moore *et al.* 2001).

IL-5, another Th2 cytokine, was also detected in mouse serum. The primary function of

IL-5 is to promote the differentiation and survival of eosinophils (Borish *et al.* 2003;

Straumann *et al.* 2013), which are usually elevated in response to allergy or parasitic

infection. Suppression of IL-5 leads to decreased presence of eosinophils and

increased parasitic burden (Korenaga *et al.* 1991). However, limited evidence exists as

to a role of IL-5 directly within the context of Lyme disease. One study demonstrated

that suppression of IL-5, in conjunction with suppression of IL-4, prior to infection led to

significantly decreased spirochete load in various target organs in Lyme disease

susceptible mice (Zeidner *et al.* 2008). In our study, as no statistically significant

differences were observed in the levels of IL-5 in serum, and as the levels of IL-5 were

relatively low, it is plausible that IL-5 is only present in the serum due to the inherent immunological bias of BALB/c mice towards a Th2 immune response and may not serve an important role in response to *B. burgdorferi* infection.

By contrast, IL-4 was the most abundant cytokine detected in mouse serum. IL-4 is the primary effector cytokine produced by Th2 cells (Watanabe *et al*. 2004). The role of IL-4 in Lyme disease progression has been extensively characterized. The notion that BALB/c mice are a Lyme arthritis-resistant mouse model has been attributed to development of a Th2 response, with IL-4 being an important cytokine for resistance (Matyniak and Reiner 1995; Keane-Myers and Nickell 1995). By contrast, subsequent studies have suggested that IL-4 is not absolutely required for resistance to arthritis development (Brown and Reiner 1999). The presence of IL-4 in BALB/c mice has been correlated with a rapid resolution of Lyme arthritis, but does not prevent the development of arthritis (Kang *et al*. 1997). Additionally, IL-4 is not believed to be essential for the control of carditis in the BALB/c mice (Satoskar *et al*. 2000). These findings demonstrate conflicting roles of IL-4 in response to infection with *B. burgdorferi*. Depletion of Treg cells did not appear to have any significant effect on the levels of IL-4 in serum; however, the presence of IL-4 suggests involvement of other types of immune cells, which could potentially have been impacted by depletion of Treg cells. IL-4 contributes to the stimulation of antibody production by B cells (Yssl *et al*. 1991), so the effect of Treg cell depletion may be visible in B cells and antibody production early in response to infection with *B. burgdorferi*.

IL-4 is present in the serum of BALB/c mice even under normal conditions. This has been corroborated by the finding that naïve CD4$^+$ T cells produce basal levels of IL-4 under normal conditions, which contributes to the Th2 polarization in BALB/c mice (Yagi *et al.* 2006). The presence of IL-4 under steady state conditions could potentially impact the development of Treg cells. In fact, Th2 and Treg cells appear to be closely related to one another. Observations in intestinal parasitic infection have suggested that the timing of exposure to IL-4 could suppress the development of Treg cells by promoting the loss of Foxp3 and the development of Th2 cells (Pelly *et al.* 2017). It has also been reported that, under certain inflammatory conditions, Treg cells lose their expression of Foxp3, which causes them to become Th2-like cells even under conditions that would normally promote the development of Th1 cells (Wan *et al.* 2007). It could be possible that Treg cells exist in low numbers in BALB/c mice due to the genetic predisposition towards a Th2-biased immune response, which could explain why few observable effects of Treg cell depletion on arthritis were observed in the mice infected with lower doses of *B. burgdorferi*. Maybe this effect could be overcome by the use of higher infectious doses in future studies.

Although the cytokine analysis did not support a role for the depletion of Treg cells on inflammatory mediators, the cytokine profile did provide further support for the Th2 bias present in BALB/c mice. Taken collectively, the effect of Treg cell depletion on borrelial load in joint and heart tissue and the lack of an observable effect of Treg cell depletion on many cytokines present in the serum suggests that Treg cells may actually have an impact on aspects of the immune response other than on Th1, Th2, or Th17 cells and

their respective cytokines. Treg cells can exert control over a variety of cell types (Arce-SIllas *et al.* 2016), so future studies could analyze the effect of Treg cell depletion on other components of the immune response, especially innate cells that are important for clearance of *B. burgdorferi*. Some of our data provide support for a role for Treg cells in the development and progression of Lyme disease; however, additional studies are needed to further analyze the role of Treg cells in the context of Lyme disease, particularly within the BALB/c mouse model.

CHAPTER 5: CONCLUSION AND FUTURE DIRECTIONS

The hypothesis for this thesis was that Treg cells control the development and progression of Lyme disease following infection with *Borrelia burgdorferi.* To test this hypothesis, two specific aims were pursued. The first specific aim focused on the development of arthritis, with the working hypothesis that Treg cell depletion would exacerbate both tibiotarsal joint swelling and arthritis. The second specific aim focused on the ability of Treg cells to control the immune response to *B. burgdorferi* infection, with the working hypothesis that Treg cell depletion would lead to increased control of bacterial dissemination and increased levels of circulating pro-inflammatory cytokines. The central hypothesis was partially supported by the trends in tibiotarsal joint swelling, certain aspects of arthritic development, and the borrelial load in joints and heart tissues observed in mice depleted of Treg cells. Importantly, our results appeared to be dependent upon the infectious doses of *B. burgdorferi* that we used.

Multiple directions could be considered when developing future experiments in BALB/c DEREG mice. Paw swelling trends, particularly those observed in mice infected with 1×10^3 *B. burgdorferi* microorganisms, provide support for extending the experimental duration beyond 35 days. Although no statistically significant differences were observed between infected DEREG mice previously administered PBS and infected DEREG mice previously administered DTx, swelling differences between infected DEREG mice previously administered DTx and infected WT mice previously administered DTx reached statistical significance by the end the of the experiment. Additionally, tibiotarsal joint swelling began to decrease in both infected DEREG mice previously administered

PBS and infected WT mice previously administered DTx, whereas the swelling

observed in infected DEREG mice previously administered DTx began to plateau. The

decrease in swelling suggests a potential resolution of disease when Treg cells were

not depleted. It is possible that depletion of Treg cells affects disease resolution in

BALB/c mice by altering the initial immune response to infection with *B. burgdorferi*,

which could then stimulate a cascade of downstream immunological effects. Future

experiments could extend the duration of the experiments beyond 35 days.

As infection with $1X10^2$ and $1X10^3$ *B. burgdorferi* appeared to be too low of infectious

doses to induce arthritis development, it may be beneficial to increase the infectious

dose in future studies. Arthritis severity correlates with increasing infectious doses (Ma

et al. 1998). In addition to increasing the infectious dose for future experiments, it would

be beneficial to determine the effect of Treg cell depletion on carditis, as carditis was

not assessed in these experiments. It has been suggested that the route of inoculation

determines the course of disease progression as spirochetes are more likely to travel to

sites proximal to the site of infection, such as the heart, rather than to distal sites, such

as the joints (Motameni *et al*. 2005). Additionally, BALB/c mice tend to develop severe

heart disease but only mild joint disease (Moody and Barthold 1998); therefore, the

effects of Treg cell depletion may be more easily observable in carditis, rather than

arthritis.

Lastly, it appeared that the depletion of Treg cells prior to infection affected some

aspects of the immune system that had downstream impacts on the course of disease

progression. The primary mechanism by which Treg cells control the immune response is by secretion of anti-inflammatory cytokines, which can act on multiple types of immune cells in multiple ways (Arce-Sillas *et al.* 2016). Other components, such as macrophages, B cells, and antibodies, have been implicated in the response to infection with *B. burgdorferi* (Barthold *et al.* 1991; McKisic and Barthold 2000; Creson *et al.* 1996), so it may be beneficial to determine the effect of Treg cell depletion on other aspects of the immune system that may be important for preventing the establishment of infection. An increase in tibiotarsal joint swelling was observed in DEREG mice administered DTx prior to infection with $1X10^2$ organisms, demonstrating support for the role of Treg cells in controlling infection. Although Treg cell depletion is only temporary in DEREG mice, depletion of Treg cells prior to infection appeared to have been sufficient to affect the initial immune response to infection. This effect then appeared to be maintained throughout the experiment, as tibiotarsal joint swelling increased consistently for the duration of the experiment and, based on the swelling trend, could have potentially continued beyond the 20 days. In future studies, additional time points could also be examined earlier during the course of infection, perhaps closer towards the initial depletion of Treg cells to account for the effect of Treg cell depletion on innate immune cells and their cytokines.

REFERENCES

Adams DA, Thomas KR, Jajosky R, Foster L, Sharp P, Onweh DH, Schley AW, Anderson WJ. 2016. Summary of Notifiable Infectious Diseases and Conditions — United States, 2014. MMWR Morb Mortal Wkly Rep **63**:1-152.

Arce-Sillas A, Alvarez-Luquin DD, Tamaya-Dominguez B, Gomez-Fuentes S, Trejo-Garcia A, Melo-Salas M, Cardenas G, Rodriguez-Ramirez J, Adalid-Peralta L. 2016. Regulatory T Cells: Molecular Actions on Effect Cells in Immune Regulation. J Immunol Research **2016**: 1-12.

Auwaerter PG, **Aucott J**, **Dumler JS**. 2004. Lyme borreliosis (Lyme disease): Molecular and cellular pathobiology and prospects for prevention, diagnosis and treatment. Expert Rev Mol Med **6**: 1–22.

Barthold SW, **Beck DS**, **Hansen GM**, **Terwilliger GA**, **Moody KD**. 1990. Lyme Borreliosis in Selected Strains and Ages of Laboratory Mice. J Infect Dis **162**: 133–138.

Barthold SW, **Persing DH**, **Armstrong AL**, **Peeples RA**. 1991. Kinetics of Borrelia burgdorferi Dissemination and Evolution of Disease After Intradermal Inoculation of Mice. Am J Pathol **139**: 263–273.

Benach JL, Fleit HB, Habicht GS. 1984. Interactions of phagocytes with the Lyme disease spirochete: role of the Fc receptor. J Infect Dis **150**: 497-507.

Bettelli E, **Carrier Y**, **Gao W**, **Korn T**, **Strom TB**, **Oukka M**, **Weiner HL**, **Kichroo VK**. 2006. Reciprocal developmental pathways for the generation of pathogenic effector T_H17 and regulatory T cells. Nature **441**: 235-238.

Blum LK, Adamska JZ, Martin DS, Rebman AW, Elliott SE, Cao RRL, Embers ME, Aucott JN, Soloski MJ, Robinson WH. 2018. Robust B Cell Responses Predict Rapid Resolution of Lyme Disease. Front Immunol **9**: 1-9.

Bockenstedt LK, **Gonzalez DG**, **Haberman AM**, **Belperron AA**. 2012. Spirochete antigens persist near cartilage after murine Lyme borreliosis therapy. J Clin Invest **122**: 2652–2660.

Brown CR, **Reiner SL**. 1999. Experimental Lyme Arthritis in the Absence of Interleukin-4 or Gamma Interferon. Infect Immun **67**: 3329–3333.

Brown JP, Zachary JF, Teuscher C Weis JJ, Wooten RM. 1999. Dual Role of Interleukin-10 in Murine Lyme Disease: Regulation of Arthritis Severity and Host Defense. Infect Immun **67**: 5142-50.

Brusko TM, **Putnam AL**, **Bluestone JA**. 2008. Human regulatory T cells: role in autoimmune disease and therapeutic opportunities. Immunol Rev **223**: 371–390.

Burchill MA, **Nardelli DT**, **England DM**, **Decoster DJ**, **Christopherson JA**, **Callister SM**, **Schell RF**. 2003. Inhibition of Interleukin-17 Prevents the Development of Arthritis in Vaccinated Mice Challenged with Borrelia burgdorferi. Infect Immun **71**: 3437–3442.

Burgdorfer W, Barbour AG, Hayes SF et al. 1982. Lyme disease-a tick-borne spirochetosis? Science **216**: 1317-1319.

Carlson D, **Hernandez J**, **Bloom BJ**, **Coburn J**, **Aversa JM**, **Steere AC**. 1999. Lack of Borrelia burgdorferi DNA in synovial samples from patients with antibiotic treatment-resistant Lyme arthritis. Arthritis Rheum **42**: 2705–2709.

Centers for Disease Control and Prevention. 2019. Lyme Disease. Date Accessed: 21 July 2019. https://www.cdc.gov/lyme/

Codolo G, **Amedei A**, **Steere AC**, **Papinutto E**, **Cappon A**, **Polenghi A**, **Benagiano M**, **Paccani SR**, **Sambri V**, **Prete G Del**, **Baldari CT**, **Zanotti G**, **Montecucco C**, **Elios MMD**, **Bernard M De**. 2008. Borrelia burgdorferi NapA – Driven Th17 Cell Inflammation in Lyme Arthritis. Arthritis Rheum **58**: 3609–3617.

Cosmi L, Liotta F, Angeli R, Mazzinghi B, Santarfasci V, Manetti R, Lasagni L, Vanini V, Romagnani P, Maggi E, Annunziato F, Romagnani S. 2004. Th2 cells are less susceptible than Th1 cells to the suppressive activity of CD25+ regulatory thymocytes because of their responsiveness to different cytokines. Blood **103**: 3117-3121.

Creson JR, Lim LC, Glowacki NJ, Callister SM, Schell RF. 1996. Detection of anti-Borrelia burgdorferi antibody responses with the borreliacidal antibody test, indirect fluorescent-antibody assay performed by flow cytometry and western immunoblotting. Clin Diagn Lab Immunol **3**: 184-190.

Curtis MW, Hahn BL, Zhang K, Li C, Robinson RT, Coburn J. 2018. Characterization of Stress and Innate Immunity Resistance of Wild-Type and Δ*p66 Borrelia burgdorferi*. Infect Immun **86**: 1-18.

Depietropaolo DL, **Powers JH**, **Gill JM**, **Foy AJ**. 2005. Diagnosis of Lyme Disease. Am Fam Physician **72**: 297–304.

de Souza MS, Smith AL, Beck DS, Terwilliger GA, Fikrig E, Barthold SW. 1993. Long-Term Study of Cell-Mediated Responses to *Borrelia burgdorferi* in the Laboratory Mouse. Infect Immun **61**: 1814-1822.

Drouin EE, **Seward RJ**, **Strle K**, **McHugh G**, **Katchar K**, **Londono D**, **Yao C**, **Costello CE**, **Steere AC**. 2013. A Novel Human Autoantigen, Endothelial Cell Growth Factor, is a Target of T and B Cell Responses in Patients with Lyme Disease. Arthritis Rheum **65**: 186-196.

Fish AE, **Pride YB**, **Pinto DS**. 2008. Lyme Carditis. Infect Dis Clin North Am **22**: 275–288.

Fishman MA, Perelson AS. 1999. Th1/Th2 differentiation and cross-regulation. Bull Math Biol **61**: 403-36.

Fontenot JD, **Gavin MA**, **Rudensky AY**. 2003. Foxp3 programs the development and function of CD4+CD25+ regulatory T cells. Nat Immunol **4**: 330-336.

Giambartolomei GH, Dennis VA, Philipp MT. 1998. Borrelia burgdorferi stimulates the production of interleukin-10 in peripheral blood mononucelar cells from uninfected humans and rhesus monkeys. Infect Immun **66**: 2691-2697.

Glickstein L, Edelstein M, Dong JZ. 2001. Gamma Interferon Is Not Required for Arthritis Resistance in the Murine Lyme Disease Model. **69**: 3737-3743.

Grimm D, Tilly K, Byram R, Stewart PE, Krum JG, Bueschel DM, Schwan TG, Policastro PF, Elias AF, Rosa PA. 2003. Outer-surface protein C of the Lyme disease spirochete: A protein induced in ticks for infection of mammals. PNAS **101**: 3142-3147.

Gross DM, **Steere AC**, **Huber BT**, **Gross DM**, **Steere AC**, **Huber BT**. 1998. T Helper 1 Response is Dominant and Localized to the Synovial Fluid in Patients with Lyme Arthritis. J Immunol **160**: 1022–1028.

Guo BP, **Norris SJ**, **Rosenberg LC**, **Hook M**. 1995. Adherence of Borrelia burgdorferi to the Proteoglycan Decorin. Infect Immun **63**: 3467–3472.

Haque A, Best SE, Amante FH. 2010. CD4+ natural regulatory T cells prevent experimental cerebral malaria via CTLA-4 when expanded in vivo. PLoS Pathog **6**: 1-14.

Hellwage J, **Meri T**, **Heikkila T**, **Alitalo A**, **Panelius J**, **Lahdenne P**, **Seppala I**, **Meri S**. 2001. The Complement Regulator Factor H Binds to the Surface Protein OspE of Borrelia burgdorferi. J Biol Chem **276**: 8427–8435.

Hildenbrand P, **Craven DE**, **Jones R**, **Nemeskal P**. 2009. Lyme Neuroborreliosis: Manifestations of a Rapidly Emerging Zoonosis. Am J Neuroradiol **30**: 1079-1087.

Hubalek Z. 2009. Epidemiology of Lyme Borreliosis. Curr Probl Dermatol **37**: 31-50.

Johanns TM, Ertelt JM, Rowe JH, Way SS. 2010. Regulatory T cell suppressive potency dictates the balance between bacterial proliferation and clearance during persistent Salmonella infection. PLoS Pathog **6**: 1-14.

Jutras BL, Lochhead RB, Kloos ZA, Biboy J, Strle K, Booth CJ, Govers SK, Gray J, Schumann P, Vollmer W, Bockenstedt LK, Steere AC, Jacobs-Wagner C. 2019. Borrelia burgdorferi peptidoglycan is a persistent antigen in patients with Lyme arthritis. PNAS **116**: 13498-13507.

Kang I, **Barthold SW**, **Persing DH**, **Bockenstedt LK**. 1997. T-Helper-Cell Cytokines in the Early Evolution of Murine Lyme Arthritis. Infect Immun **65**: 3107–3111.

Keane-Meyers A, Nickell SP. 1995. T cell subset-dependent modulation of immunity to *Borrelia burgdorferi* in mice. J. Immunol. **154**: 1770-1776.

Korenaga M, Hitoshi Y, Yamaguchi N, Sato Y, Takatsu K, Tada I. 1991. The role of interleukin-5 in protective immunity to Strongyloides venezuelensis infection in mice. Immunol **72**: 502-507.

Kotloski NJ, **Nardelli DT**, **Peterson SH**, **Torrealba JR**, **Warner TF**, **Callister SM**, **Schell RF**. 2008. Interleukin-23 Is Required for Development of Arthritis in Mice Vaccinated and Challenged with Borrelia Species. Clin Vaccine Immunol **15**: 1199–1207.

Kugeler KJ, Farley GM, Forrester JD, Mead PS. 2015. Geographic Distribution andn Expansion of Human Lyme Disease, United States. Emerg Infect Dis **8**: 1455-1457.

Lahl K, **Loddenkemper C**, **Drouin C**, **Freyer J**, **Arnason J**, **Eberl G**, **Hamann A**, **Wagner H**, **Huehn J**, **Sparwasser T**. 2007. Selective depletion of Foxp3+ regulatory T cells induces a scrufy-like disease. J Exp Med **204**: 57-63.

Lahl K, Sparwasser T. 2011. In Vivo Depletion of FoxP3+ Tregs Using the DEREG Mouse Model. Methods Mol Biol **707**: 157-172.

Lanteri MC, O'Brien KM, Purtha WE. 2009. Tregs control the development of symptomatic West Nile virus infection in humans and mice. J Clin Investig **119**: 3266–3277.

Liu Y, **Zhang P**, **Li J**, **Kulkami AB**, **Perroche S**, **Chen W**. 2008. A critical function for TGF-β signaling in the development of natural CD4+CD25+Foxp3+ regulatory T cells. Nat Immunol **9**: 632-640.

Lund JM, Hsing L, Pham TT, Rudensky AY. 2008. Coordination of early protective immunity to viral infection by regulatory T cells. Science **320**: 1220–1224.

Ma Y, **Seiler KP**, **Eichwald EJ**, **Weis JH**, **Teuscher C**, **Weis JJ**. 1998. Distinct Characteristics of Resistance to Borrelia burgdorferi-Induced Arthritis in C57BL/6N Mice. Infect Immun **66**: 161–168.

Matyniak JE, **Reiner SL**. 1995. T Helper Phenotype and Genetic Susceptibility in Experimental Lyme Disease. J Exp Med **181**: 1251–1254.

Mayer CT, Lahl K, Milanez-Almeida P, Watts D, Dittmer U, Fyhrquist N, Huehn J, Kopf M, Kretschmer K, Rouse B, Sparwasser T. 2014. Advantages of Foxp3$^+$ regulatory T cell depletion using DEREG mice. Immun Inflamm Dis **2**: 162-165.

McKisic MD, Barthold SW. 2000. T-cell-independent responses to Borrelia burgdorferi are critical for protective immunity and resolution of Lyme disease. Infect Immun **68**: 5190-5197.

Moody KD, Barthold SW. 1998. Lyme Borreliosis in Laboratory Mice. Lab Anim Sci **2**: 168-171.

Moore KW, Malefyt R de W, Coffman RL, O-Garra A. 2001. Interleukin-10 and the interleukin-10 receptor. Annu Rev Immunol **19**: 683-765.

Motameni AR, Bates TC, Juncadella IJ, Petty C, Hedrick MN, Anguita J. 2005. Distinct bacterial dissemination and disease outcome in mice subcutaneously infected with Borrelia burgdorferi in the midline of the back and the footpad. FEMS Immunol Med Microbiol **45**: 279-284.

Nardelli DT, **Burchill MA**, **England DM**, **Torrealba J**, **Callister SM**, **Schell RF**. 2004. Association of CD4+ CD25+ T Cells with Prevention of Severe Destructive Arthritis in Borrelia burgdorferi-Vaccinated and Challenged Gamma Interferon-Deficient Mice Treated with Anti-Interleukin-17 Antibody. Clin Diagn Lab Immunol **11**: 1075–1084.

Nardelli DT, **Cloute JP**, **Luk KHK**, **Torrealba J**, **Warner TF**, **Callister SM**, **Schell RF**. 2005. CD4 + CD25 + T Cells Prevent Arthritis Associated with Borrelia Vaccination and Infection. Clin Diagn Lab Immunol **12**: 786–792.

Nardelli DT, **Warner TF**, **Callister SM**, **Schell RF**. 2006. Anti-CD25 Antibody Treatment of Mice Vaccinated and Challenged With Borrelia spp. Does Not Exacerbate Arthritis but Inhibits Borreliacidal Antibody Production. Clin Vaccine Immunol **13**: 884-891.

Nau R, **Christen H-J**, **Eiffert H**. 2009. Lyme Disease-Current State of Knowledge. Dtsch Arztebl Int **106**: 72-82.

Nocton JJ, **Dressler F**, **Rutledge BJ**, **Rhys PN**, **Persing DH**, **Steere AC**. 1994. Detection of Borrelia burgdorferi DNA by polymerase chain reaction in synovial fluid of patients with Lyme arthritis. N Engl J Med **330**: 229–234.

Oldenhove G, Bouladoux N, Wohlfert EA. 2009. Decrease of Foxp3+ Treg cell number and acquisition of effector cell phenotype during lethal infection. Immunity **31**: 772–86.

Pal U, **Silva AM De**, **Montgomery RR**, **Fish D**, **Anguita J**, **Anderson JF**, **Lobet Y**, **Fikrig E**. 2000. Attachment of Borrelia burgdorferi within Ixodes scapularis mediated by outer surface protein A. J Clin Invest **106**: 561–569.

Pandiyan P, Conti HR, Zheng L. 2011. CD4+ CD25+ Foxp3+ regulatory T cells promote Th17 cells in vitro and enhance host resistance in mouse Candida albicans Th17 cell infection model. Immunity **34**: 422–34.

Pelly VS, Coomes SM, Kannan Y, Gialitakis M, Entwistle LJ, Perez-Lloret J, Czieso S, Okoye IS, Ruckerl D, Allen JE, Brombacher F, Wilson MS. 2017. Interleukin 4 promotes the development of ex-Foxp3 Th2 cells during immunity to intestinal helminths. J Exp Med **214**: 1809-1826.

Probert WS, **Johnson BJB**. 1998. Identification of a 47 kDa fibronectin-binding protein expressed by Borrelia burgdorferi isolate B31. Mol Microbiol **30**: 1003–1015.

Ristow LC, **Miller HE**, **Padmore LJ**, **Chettri R**, **Salzman N**, **Caimano MJ**, **Rosa PA**, **Coburn J**. 2012. The β_3-integrin ligand of Borrelia burgdorferi is critical for infection of mice but not ticks. Molec Micro **85**: 1105-1118.

Rowe JH, Ertelt JM, Aguilera MN, Farrar MA, Way SS. 2011. Foxp3+ regulatory T cell expansion required for sustaining pregnancy compromises host defense against prenatal bacterial pathogens. Cell Host Microbe **10**: 54–64.

Sakaguchi S, **Yamaguchi T**, **Nomura T**, **Ono M**. 2008. Regulatory T Cells and Immune Tolerance. Cell **133**: 775–787.

Sanchez E, **Vannier E**, **Wormser GP**, **Hu LT**. 2016. Diagnosis, Treatment, and Prevention of Lyme Disease, Human Granulocytic Anaplasmosis, and Babesiosis: A Review. JAMA **315**: 1767-1777.

Sanjabi S, **Zenewicz L**, **Kamanaka M**, **Flavell R**. 2010. Anti- and Pro-inflammatory Roles of TGF-β, IL-10, and IL-22 In Immunity and Autoimmunity. Curr Opin Pharmacol **9**: 447–453.

Satoskar AR, Elizondo J, Monteforte GM, Stamm LM, Bluethmann H, Katavolos P, Telford III SR. 2000. Interleukin-4-deficient BALB/c mice develop an enhanced Th1-like response but control cardiac inflammation following *Borrelia burgdorferi* infection. FEMS Microbiol Letters **183**: 319-325.

Scheffold N, **Herkommer B**, **Kandolf R**, **May AE**. 2015. Lyme Carditis — Diagnosis, Treatment and Prognosis. Dtsch Arztebl Int **112**: 202–208.

Schwan T, **Piesman J**. 2000. Temporal Changes in Outer Surface Proteins A and C of the Lyme Disease-Associated Spirochete, Borrelia burgdorferi, during the Chain of Infection in Ticks and Mice. J Clin Microbiol **38**: 382–388.

Schwan T, **Piesman J**, **Golde WT**, **Dolan MC**, **Rosa PA**. 1995. Induction of an outer surface protein on Borrelia burgdorferi during tick feeding. Proc Natl Acad Sci USA **92**: 2909–2913.

Shen S, **Shin JJ**, **Strle K**, **McHugh G**, **Li X**, **Glickstein LJ**, **Drouin EE**, **Steere AC**. 2010. Treg Cell Numbers and Function in Patients With Antibiotic-Refractory or Antibiotic-Responsive Lyme Arthritis. Arthritis Rheum **62**: 2127–2137.

Stanek G, **Wormser GP**, **Gray J**, **Strle F**. 2011. Lyme borreliosis. Lancet **6376**: 1–14.

Steere AC, **Coburn J**, **Glickstein L**. 2004. The emergence of Lyme disease. J Clin Invest **113**: 1093–1101.

Steere AC, **Glickstein L**. 2004. Elucidation of Lyme Arthritis. Nat Rev Immunol **4**: 143–152.

Straumann A. 2013. Antieosinophil Therapeutics. Eosinophils in Health and Disease. Academic Press, Orlando, p. 577-605.

Strle F, **Stanek G.** 2009. Clinical Manifestations and Diagnosis of Lyme Borreliosis. Curr Probl Dermatol **37**: 51-110.

Strle K, **Stupica D**, **Drouin EE**, **Steere AC**. 2014. Elevated Levels of IL-23 in a Subset of Patients with Post-Lyme Disease Symptoms Following Erythema Migrans. Clin Infec Dis **58**: 372-380.

Tilly K, **Krum JG**, **Bestor A**, **Jewett MW**, **Grimm D**, **Bueschel D**, **Byram R**, **Dorward D**, **VanRaden MJ**, **Stewart P**, **Rosa P.** 2006. Borrelia burgdorferi OspC Protein Required Exclusively in a Crucial Early Stage of Mammalian Infection. Infect Immun **74**: 3554-3564.

Vudattu NK, **Strle K**, **Steere AC**, **Drouin EE**. 2013. Dysregulation of CD4+CD25 high T Cells in the Synovial Fluid of Patients With Antibiotic-Refractory Lyme Arthritis. Arthritis Rheum **65**: 1643–1653.

Wan YY, Flavell RA. 2007. Regulatory T-cell functions are subverted and converted owing to attenuated Foxp3 expression. Nature **445**: 766-770.

Watanabe H, Numata K, Ito T, Takagi K, Matsukawa A. 2004. Innate Immune Response in Th1- and Th2- Dominant Mouse Strains. Shock **22**: 460-466.

Wormser GP, **Dattwyler RJ**, **Shapiro ED**, **Halperin JJ**, **Steere AC**, **Klempner MS**, **Krause PJ**, **Bakken JS**, **Strle F**, **Stanek G**, **Bockenstedt L**, **Fish D**, **Dumler JS**, **Nadelman RB**. 2006. The Clinical Assessment, Treatment, and Prevention of Lyme Disease, Human Granulocytic Anaplasmosis, and Babesiosis: Clinical Practice Guidelines by the Infectious Diseases Society of America. Clin Infect Dis **43**: 1089–1134.

Wormser GP, **Nadelmann RB**, **Schwartz I**. 2012. The amber theory of Lyme arthritis: initial description and clinical implications. Clin Rheumatol **31**: 989-994.

Wright WF, **Riedel DJ**, **Talwani R**, **Gilliam BL**. 2012. Diagnosis and Management of Lyme Disease. Am Fam Physician **85**: 1086–1093.

Yagi J, Arimura Y, Takatori H, Nakajima H, Iwamoto I, Uchiyama T. 2006. Genetic background influences T_h cell differentiation by controlling the capacity for IL-2-induced IL-4 production by naïve CD4+ T cells. Int Immunol **18**: 1681-1690.

Yang L, Weis JH, Eichwald E, Kolbert CP, Persing DH, Weis JJ. 1994. Heritable Susceptibility to Severe *Borrelia burgdorferi*-Induced Arthritis is Dominant and Is Associated with Persistence of Large Numbers of Spirochetes in Tissues. Infect Immun **62**: 492-500.

Yoshimura A, Wakabayashi Y, Mori T. 2010. Cellular and molecular basis for the regulation of inflammation by TGF-beta. J Biochem **147**: 781-792.

Yssl H, Shanafelt MC, Soderberg C, Schneider PV, Anzola J, Peltz G. 1991. *Borrelia burdorferi* activates a T helper type 1-like T cell subset in Lyme arthritis. J Exp Med **174**: 593-601.

Zeidner N, **Mbow ML**, **Dolan M**, **Massung R**, **Baca E**, **Piesman J**. 1997. Effects of Ixodes scapularis and Borrelia burgdorferi on Modulation of the Host Immune Response : Induction of a TH2 Cytokine Response in Lyme Disease-Susceptible (C3H/HeJ) Mice but not in Disease-Resistant (BALB/c) Mice. Infection **65**: 3100–3106.